12-2013

Spectroscopic, Thermal, and Physical Analysis of the Raw Materials in Europium Doped Cesium Strontium Iodide Scintillator

Bonnie Dell Blalock
University of Tennessee - Knoxville, bblaloc3@utk.edu

To the Graduate Council:

I am submitting herewith a thesis written by Bonnie Dell Blalock entitled "Spectroscopic, Thermal, and Physical Analysis of the Raw Materials in Europium Doped Cesium Strontium Iodide Scintillator." I have examined the final electronic copy of this thesis for form and content and recommend that it be accepted in partial fulfillment of the requirements for the degree of Master of Science, with a major in Materials Science and Engineering.

Mariya Zhuravleva, Major Professor

We have read this thesis and recommend its acceptance:

Charles L. Melcher, Claudia J. Rawn

Accepted for the Council:
Carolyn R. Hodges

Vice Provost and Dean of the Graduate School

(Original signatures are on file with official student records.)

Spectroscopic, Thermal, and Physical Analysis of the Raw Materials in Europium Doped Cesium Strontium Iodide Scintillator

A Thesis Presented for the
Master of Science Degree
The University of Tennessee, Knoxville

Bonnie Dell Blalock
December 2013

ACKNOWLEDGMENTS

I would like to acknowledge the support provided by the US Department of Homeland Security, Domestic Nuclear Detection Office under grant # 2012-DN-077-ARI067-02 that made this work possible. I would also like to thank the Center for Materials Processing for their contribution to funding me during my graduate studies. Additional thanks goes to Siemens Medical Solutions for helping provide some of the funding to keep the SMRC running.

There are a great number of people who I would like to thank for their moral support. I would like to thank all of the people that I have had the pleasure of working with over the years at the Scintillation Materials Research Center. Many thanks goes to Dr. Harold Rothfuss and Dr. Kan Yang, who on my very first day working in the glove box came to my aide, and who patiently took the time to introduce me to the wonderful world of the growth and characterization of scintillation materials. To Dr. Jon Peak, Paul Cutler, Brandon Goodwin, John Bohling, Kurt Johanns, Breanna Harvell, Brett Lewis, and Aaron Hall for helping me along the way in my early years with the SMRC. I would like to express a heartfelt appreciation for my dear friend Hua Wei, who has been an invaluable resource for all things. To all of my fellow lab-mates throughout the years, including Fang Meng, Will McAlexander, Adam Lindsey, Luis Stand, Dr. Mohit Tyagi, Samuel Donnald, Chris Hobbs, Victoria Martin, and Gigi Loi, I thoroughly enjoyed working with each one of you, and I feel fortunate that I have met all of you. I would also like to thank Brittany Brown for her assistance with the thermal analysis measurements for this work.

Many thanks go to Dr. Benson and Ryan Hammonds for their time and discussion and allowing my use of the Biorad FTS 6000 that was used to measure the IR spectra. Likewise, additional thanks goes to Dr. John Auxier II, and Dr. George Schweitzer for the many useful conversations that I have had with you at certain points along this process. I would also like to thank Art Pratt and Bo Bishop for using their skilled hands to fashion many of the quartz ampoules that I have used over my years at the SMRC.

I would like to thank Lars Eriksson for always having a smile on his face when I see him in the lab. To my dear mentor Merry Koschan who has taught me many things about our work, and life in general, thanks for letting me bend your ear often, you have been an inspiration.

To all of my committee members, I am thankful for your assistance along the way, and for agreeing to be on my committee. Dr. Claudia Rawn, you were right about the SMRC being a good place to work, thank you so much for suggesting that I get into contact with this group, that suggestion truly changed my life. Dr. Chuck Melcher, thank you for being open to letting a gal like me into this lab, the opportunity to work with this group has been an exceptional experience.

Dr. Mariya Zhuravleva, you have been a tremendous help throughout my undergraduate and graduate studies. I really value the time that you have spent with me, beginning with walking me through preparing stoichiometric mixtures, and your continued efforts to share your knowledge with me when I was having trouble. You have given me an education that not many people have, and I hope that you know that I am appreciative of that. You have steered me in the right direction at all times, and have encouraged me to strive to do better.

Many thanks are due to my family and friends, who have stood on the sidelines cheering me on all the way. To my brothers, thanks for providing me with a good laugh when I needed it most. Gram Barbara, thank you for sharing your wisdom about life with me, and always being able to hear me out when I need someone to talk to. Aunt Becca, I literally would not be here without your help (you know what you did), thank you. Mom, Dad, I think we all know that I could not have made it this far without your assistance. I would like to especially thank my Mom for inspiring me to keep moving forward, no matter how hard the road ahead is, your example has kept me going. Dad, thanks for being a Biomed Tech when I was a kid, and taking me to work with you sometimes, I really do think it helped me fall in love with science at a young age. To my dear young man, Brodie, you helped me wake up and push for a better life, you may not understand it right now, but I think you will when you get older. To my loving partner, Franklin, I hope that you know how much your support has meant to me through these years. Thanks for geeking out with me and lifting me up when I needed you to.

ABSTRACT

Scintillators are widely used in homeland security applications that utilize gamma-ray spectroscopy. An ideal scintillator for this purpose should possess a high effective atomic number, high light yield, and good energy resolution. The scintillator $CsSrI_3$: Eu [cesium strontium iodide: europium], recently developed at the Scintillation Materials Research Center, has excellent properties. Recent efforts have been made to evaluate the basic thermal properties and IR spectra of the compound's raw materials as part of a project to improve the quality of grown crystals. Fourier transform infrared spectroscopy of high purity anhydrous CsI [cesium iodide], SrI_2 [strontium iodide], and EuI_2 [europium iodide] raw materials revealed the presence of oxygen and moisture impurities. The presence of the hydroxyl impurity is particularly detrimental to $CsSrI_3$: Eu [cesium strontium iodide: europium] because it is hygroscopic, and can have a deleterious effect on the overall crystal quality. Even though the as-received raw materials are anhydrous, they contain some residual hydroxyl impurities, and benefit from a drying procedure. It is important to know how the raw materials used for this compound behave as a function of temperature so that the best possible drying conditions can be discovered. Differential scanning calorimetry and thermogravimetric analysis were used in conjunction to determine optimal drying conditions. The hygroscopicity of the raw materials was also determined. Multiple samples were synthesized to study the effects of drying on this scintillator. This study allows a broader understanding of the challenges to overcome in order to improve this promising scintillation material.

TABLE OF CONTENTS

LIST OF TABLES

LIST OF FIGURES

CHAPTER 1 INTRODUCTION

Scintillators are materials that have the ability to convert energy from ionizing radiation into pulses of light commonly known as photons. These materials have allowed the advancement in technology of homeland security, high energy physics and medical imaging applications. Scintillation materials can either be organic or inorganic and can exist in the solid, liquid, or gaseous states. This thesis presents the study of the pre-synthesis processing of as-received materials that are used in the synthesis of the crystalline inorganic metal halide scintillator $CsSrI_3$: Eu.

A discussion about the qualifications of a good scintillator material is necessary to provide insight as to why $CsSrI_3$: Eu was studied. A review of the requirements of an inorganic scintillation material based on the different types of radiation detector application is provided in the following section.

1.1 Requirements of ideal scintillators

In order to correctly identify what kinds of applications a scintillator will be suitable for, the advantages and disadvantages have to be considered. In general, an ideal scintillator is one that has the following properties:

1. Converts the kinetic energy of charged particles into detectable light with high scintillation efficiency.
2. Spatial resolution and sensitivity of detectors in nuclear detection devices require sufficient energy resolution.
3. The medium should be transparent to the wavelength of its own emission for good light collection.
4. The decay time of the induced luminescence should be short so that fast signal pulses can be generated.
5. The material should be of good optical quality and subject to manufacture in sizes large enough to be of interest as a particular detector.

6. Its index of refraction should be near that of glass (~1.5) to permit efficient coupling of the scintillation light to a photomultiplier tube or other light sensor [1].

During metal halide crystal growth, it is important to be aware of all of the aforementioned qualities. The crystal grower should be aware of how unintentional impurities affect these properties so that suitable procedures can be implemented to preserve the desired scintillation characteristics. The introduction of unintended impurities into the scintillator increases the potential of interfering with the luminescence center in such a way that it detracts from the desired scintillation properties which will be examined throughout this work. Further discussion is restricted to an overview of how different inorganic scintillators satisfy these properties according to various applications.

1.1.1. Scintillator applications requirements

The requirements of a scintillator to detect □-rays differ based on the application. In order to detect high energy □-rays, a scintillator must be sufficiently dense (~5 $g \cdot cm^{-3}$) to ensure adequate stopping power for the incoming ionizing radiation [2]. Dense scintillators also enjoy the benefit of leading to the development of a more compact detector, which lends itself to being a more cost effectively produced material. Additionally, scintillators used in particle physics experiments found at facilities like Conseil Européen pour la Recherche Nucléaire (CERN) need to have fast decay times (~25 ns) [2] so that multiple events can be detected. The decay time of a scintillator determines how quickly separate interactions of radiation with a scintillator can be recorded.

As homeland security concerns continue to rise due to the adverse global political climate, there has been an increased emphasis on industry for the development of radiation detection devices. High light yield and good energy resolution are necessary to achieve the level of spatial resolution and sensitivity of the detectors used in nuclear detection devices used at border crossings and cargo ports. Energy resolution is the most important consideration for homeland security applications as this property determines

how good a scintillator is at detecting weak sources of discrete energies that will allow the determination of what type of radiation source is being detected [1]. There are many sources of naturally occurring radioisotopes, such as potassium-40 (^{40}K) that is found in foods, animals and humans. Therefore it is important for the radiation detector to identify the radionuclides specific to those found in nuclear and radiological weapons, and in order to do so, the energy resolution must be adequate.

In applications where timing is an important consideration, like positron emission tomography (PET), fast, single component decay times are desirable to prevent dead time losses. Although Eu^{2+} activated scintillators have slower decay times than other rare-earth activated scintillators, some have other properties that make them worthwhile to study. For instance, SrI_2: Eu is a promising scintillator because of its excellent energy resolution and high light yield, despite having a longer decay time of 1.5 μs [3]. Later, in this chapter, the favorable scintillation properties, such as high light yield and good energy resolution, of $CsSrI_3$: Eu will be discussed. An activated scintillator, such as SrI_2: Eu and $CsSrI_3$: Eu, are compounds that require an intentional impurity to be added to the matrix to produce the luminescence center that makes the material scintillate.

1.2 Scintillation mechanism in activated scintillators

Every material has its own unique electronic band structure as a result of its crystal lattice. As for most scintillation materials, the electronic band structure resembles that of an insulating material in which the valence band is completely filled with electrons that are bound at lattice sites. Meanwhile the conduction band remains empty until electrons from the valence band have been excited with a sufficient amount of energy, which then allows the electrons to move freely throughout the crystal. The band of energies between the valence and conduction bands is referred to as the forbidden gap where electrons will scarcely be found. A small amount of an activator is commonly required to be incorporated into the host matrix in order to create new energy states within the forbidden gap. Provided a suitable activator is chosen for a particular host

material, ultra-violet (UV) or visible photon will be produced. The scintillation process from start to finish can be described as follows:

1. The scintillator material has bound electrons in the valence band.
2. Incident ionizing radiation with sufficient energy will interact with the scintillator causing the excitation of electrons from the valence band into the conduction band. A positively charged hole is created in the place within the valence band where the electron was previous to excitation. The electron-hole pair is also referred to as an exciton.
3. The hole and electron pair will migrate in the valence and conduction bands respectively until they reach an activator site.
4. The hole ionizes the activator site, and the electron will roam the conduction band until it encounters an ionized activator site where it will then migrate.
5. Provided the activator site is then one in which the excited configuration allows transitions down to the ground state, de-excitation will occur and photons will be created [1].

Figure 1 demonstrates this phenomenon. The allowable transition of Eu^{2+} activated scintillators typically display a single peak in the luminescence emission spectra that is attributed to the 5d – 4f transition with a lifetime on the order of microseconds [4-11].

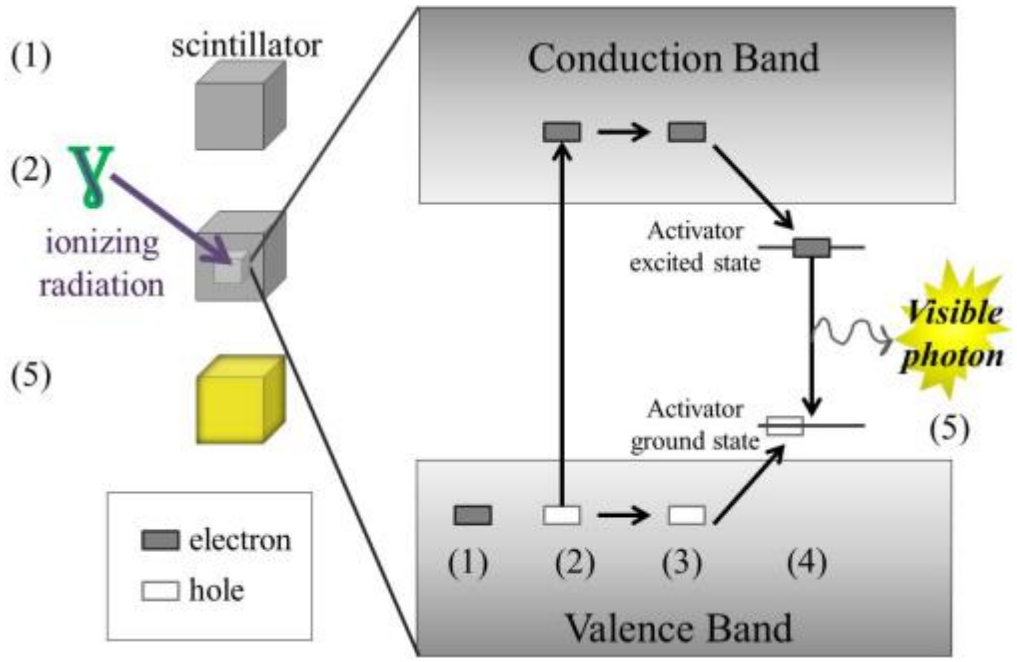

Figure 1. Simple diagram of a scintillation process in inorganic scintillators: (1) a scintillator has bound electrons in the valence band, (2) incident ionizing radiation excites an electron from the valence to the conduction band, a hole remains in the valence band, (3) the hole and electron roam the valence and conduction bands respectively in search of an activator site, (4) the hole ionizes the activator site while the electron neutralizes it, (5) de-excitation occurs and a photon is seen and the scintillator luminesces.

1.3 Metal halide scintillators

Metal halides are a class of scintillators that are characteristic of having a metal or metals, such as Cs and Sr that are ionically bonded to a halide. Halides being found in column VII of the periodic table, with the most common being fluorine, chlorine, bromine, and iodine. There are quite a few excellent properties of the metal halide scintillators. They commonly have melting temperatures that are lower than 1000°C which lend them to a possibility of being more cost effective than those with higher melting temperature oxide scintillators such as lutetium oxyorthosilicate (LSO) and gadolinium orthosilicate (GSO) [12]. What is more, these metal halide scintillation materials include some of the most proportional and luminescent properties, with good energy resolution, and are found in the inorganic variety of scintillator, such as SrI_2: Eu,

$CsBa_2I_5$: Eu, BaBrI: Eu, BaClI: Eu, and $LaBr_3$: Ce [4-11, 13]. A comparison of these scintillation properties of these materials is provided in the section discussing the development of $CsSrI_3$: Eu.

While these materials have some of the most desirable qualities of a scintillator, some of them also possess one of the most significant setbacks. Both SrI_2: Eu and $LaBr_3$: Ce are known to be hygroscopic, or readily absorbing moisture, and as such require careful attention to both pre- and post- processing. The damaging effects on the scintillation properties of hygroscopic metal halide scintillators will be discussed further later in this chapter.

1.4 Crystalline metal halide scintillator synthesis

Synthesis of inorganic scintillators is a varied process. Controlled synthesis of the dried materials can be achieved in a multi-zone furnace. Multi-zone furnaces are commonly employed to synthesize single crystalline metal halide inorganic scintillators in which two different modes of melt growth take place. The Vertical Gradient Freeze method is a growth technique that requires many heating zones within the furnace to precisely control the thermal gradient throughout the length of the furnace. The furnace is raised to the appropriate temperature to melt the raw materials in an ampoule and mix them thoroughly, and then the bottom portion of the furnace is lowered to a cooler temperature to induce crystallization. The ampoule remains in a fixed position throughout this process while the temperature profile changes toward the lower temperature [14]. The Bridgman method employs a stable gradient throughout the furnace length while the charge translates through the stationary temperature profile [14]. Gradient freeze methods enjoy the advantage over the Bridgman technique in that the charge does not have to move through the furnace with the aid of a translation mechanism. Hence the samples undergo less vibration when being grown by the gradient methods as opposed to the Bridgman method.

Melt synthesis is commonly used to produce polycrystalline scintillator samples that can be obtained more quickly than the gradient freeze and Bridgman methods. A

clamshell furnace can be employed for rapid synthesis in which the material is heated to the point of melting and then cooled to room temperature. A polycrystalline solid that is produced via the rapid melt-synthesis method is capable of having its material properties characterized. While the choice of the growth technique is important, there are other factors of scintillator synthesis that must be considered. An evaluation of what type of starting materials used to synthesize scintillators is discussed.

1.4.1 Synthesis of starting materials

Metal halide scintillators can be made from starting materials such as MCO_3 (M stands for metal) and/ or hydrated metal halides starting materials provided that a heating treatment with or without a scavenger is employed [15,16]. A scavenger is a substance added to a chemical reaction or mixture to counteract the effect of impurities, or undesired reactions. Some of the possible chemical reactions used to synthesize metal halide starting materials are listed below in equations 1-4.

$$MCO_3 + 2\ HI \rightarrow MI_2 + H_2O + CO_2 \text{ (eq. 1)}$$
$$MH_2 + 2\ NH_4I \rightarrow MI_2 + 2\ NH_3 + H_2 \text{ (eq. 2)}$$
$$MOH + HI \rightarrow MI + H_2O \text{ (eq. 3)}$$
$$2\ M + I_2 \rightarrow 2\ MI \text{ (eq. 4)}$$

The chemical reactions in equations 1-3 all have additional products that will have to be separated from the desired metal halide product. The starting materials typically used for crystal growth of halide scintillators are anhydrous metal halides with a purity of at least 99.99 %. Anhydrous raw materials are thought to have an advantage over hydrates because they do not require additional processing to remove water impurities. As many of the metal halide raw materials are hygroscopic, handling of the materials is done in a dry environment, typically on the order of 1 part per million (ppm) moisture and oxygen content. Raw materials are typically loaded into quartz ampoules, dried under a vacuum, and sealed in an attempt to prevent the incorporation of unintentional impurities.

1.5 The effects of unintentional impurities in inorganic scintillators

Upon reviewing the requirements of an ideal scintillator, it is clear that the desired qualities for radiation detection include, but are not limited to, efficient light production, and good optical quality, both of which can be negatively affected by the introduction of unintentional impurities into the scintillator. For instance, the presence of an oxygen or moisture impurities group in a scintillation material can provide an efficient non-radiative decay channel for excited impurities, thus quenching emission. Incorporation of unintentional impurities can also lead to cracking of a crystal [12]. As a result, special pre- and post- synthesis measures are required to protect the scintillator from losing its desirable scintillation properties. A discussion of some of the issues posed by these impurities is necessary to provide the basis for the properties studied in this research.

The decomposition and displacement of rare earth and alkaline metal halides is a concern for producers of scintillators as it can cause damaging effects on the scintillation properties. Reaction 5 is of significant note, as the formation of an oxyhalide becomes evident. Not only will the rare earth oxyhalide potentially cause the crystal to adhere to the ampoule wall during growth [9], but it can also quench the light yield. For the alkaline metal halide SrI_2, it has been observed that material will turn yellow in the presence of air, and in the presence of heat will decompose to form strontium oxide and iodine as demonstrated in equation 6 [17]. Certain metal halides have a reputation for being reactive in air and can absorb moisture, and oxygen in standard room temperature and humidity conditions. The following chemical reactions demonstrate how the starting materials may decompose if in the presence of oxygen or moisture.

$$2\ MI_2 + O_2 \rightarrow 2\ MOI + I_2 \text{ (eq. 5)}$$

$$2\ MI_2 + O_2 \xrightarrow{heat} 2\ MO + 2I_2 \text{ (eq. 6)}$$

$$MI_2 + H_2O \xrightarrow{heat} MO + 2\ HI \text{ (eq. 7)}$$

$$MI_2 + H_2O \xrightarrow{heat} MO + I_2 + H_2 \text{ (eq. 8)}$$

$$MI_2 + 2\ H_2O \xrightarrow{heat} M(OH)_2 + 2\ HI \text{ (eq.9)}$$

As a means of illustrating how significant the quenching can be, consider SrI_2: Eu. The material was patented in 1968, but it was not studied thoroughly directly after its invention, the light yield was ~30,000 ph/MeV [15]. The starting materials used at that time were quite different than the materials used today; the purity of the materials has improved tremendously. By 2010 the SrI_2: Eu scintillator had been revisited, and a light yield of >100,000 photons per megaelectron-volt (ph/MeV) has since then been obtained [3]. An improvement in the energy resolution was also noted. It is plausible that the purity of the raw materials used to synthesize SrI_2: Eu had some influence on the improvement of the light output, especially if the unintentional impurities were incorporated into the luminescence centers. Reations 7-9 demonstrate what could happen to the synthesized scintillator from hydrated starting materials. It is clear that the disassociation of the metal halide would likely occur, and lead to interference of the scintillation process. Thus, it becomes clear that preventative measures such as a drying procedure is necessary, which is a process that is considered further in section 1.8. Evidence of the creation of oxygen containing defects in undoped and Eu doped BaBrCl has been presented at many conferences and demonstrates the effect of the oxygen defect luminescence in the radioluminescence spectra [18-19]. Other methods are used to determine the purity of raw materials.

1.5.1 Methods of impurity analysis

It is desirable to be able to procure starting materials that meet the necessary purity standards, in order to use as received. A certificate of analysis is supplied with the materials that disclose the trace metallic impurities (TMI) as determined by the manufacturer. It is important to note that the rare-earth containing metal halides are considered some of the most challenging materials to analyze. Some of the more popular impurity analysis techniques include chemical, gravimetric, volumetric, and optical methods [20]. In classical gravimetric analysis, a constituent component of material can be converted to an insoluble precipitate that is weighed. While this technique is accurate, it can only provide analysis of a small number of groups at a time. Volumetric (also

referred to as titrimetric) analysis determines the unknown concentration of a sample by reacting the substance with an appropriate reagent, and the volume of solution needed for complete reaction is determined. Optical methods can be dependent on the absorption of energy at a given wavelength of a material or the emission of energy at a given wavelength. Visible, ultra violet (UV), infrared, and atomic absorption spectroscopy are examples of optical methods. One of the spectroscopic methods used to determine the TMI in metal halides from Sigma Aldrich is inductively coupled plasma mass spectrometry (ICP-MS) [21]. The ICP-MS technique offers extremely low detection limits in the parts per trillion (ppt) up to the ppm range [22]. As the name implies, samples are evaluated by ionizing a sample with an argon plasma and using a mass spectrometer to measure the produced ions and quantify them. A technique using infrared spectroscopy can also be used to observe an unintentional impurity in a host material. In comparison with gravimetric analysis, infrared spectroscopy can provide more information in one measurement since the technique is sensitive to the molecular vibrations of all the ions in a material, as opposed to only being able to detect one functional group at a time. For the purpose of this work, infrared spectroscopy was sufficient to detect impurities in the as-received raw materials.

1.5.1.1 Infrared spectroscopy

Infrared (IR) spectroscopy can be used to study chemicals and identify molecular bonds. Every type of bond or group has a specific frequency in which it absorbs radiation and will vibrate creating characteristic absorption peaks on the electromagnetic (EM) spectrum that are representative of that functional group that has experienced a change in their dipole moments. Molecular vibrations arise from IR radiation interacting with the chemical bonds in a functional group. The radiation will cause stretching (both symmetric or asymmetric) of the bonds, which are generally observed between 4000 and 2500 cm^{-1}. Similarly, the IR radiation will induce bending modes in the molecule that are observed from ~2500 cm^{-1} to 500 cm^{-1}.

Atomic impurity ions that are included in a crystal will change the absorption spectrum of the original material. In inorganic materials the -OH stretching peak is

present in the 3550-3200 cm^{-1} and the vibration caused by HOH bending is found ~1630-1600 cm^{-1} in the mid-infrared region of the EM spectrum [23]. The instrumentation of the Fourier transform infrared spectrometer will be discussed in the next chapter. The detection of oxygen and moisture impurities in NaI, KI, and many other alkali halide crystals have been reported [24]. In 2002 Fourier transform infrared spectroscopy (FT-IR) was used to study the oxygen and moisture found in Ce and Gd doped silicate glasses that were intended for scintillation applications [25]. Scintillator crystals, such as LiF doped with different polyvalent cations and CsI: Eu have also been studied with FT-IR and have observed oxygen and moisture impurities [26-27].

1.6 Determination of drying procedures

The ultimate goal of this research is to optimize the pre-synthesis process so that a limited amount of impurities are incorporated into the scintillator. Many metal halide scintillators and the starting materials used to synthesize them are known to interact with moisture and O_2 as seen in the reactions in equations 5-9 in section 1.5. While water has a known boiling temperature above 100°C, it is reasonable to assume that the temperature required to remove the moisture adsorbed in a metal halide that has experienced a chemical reaction would be different. Thermoanalytical techniques can be used to observe the precise temperature that volatilization in metal halide raw materials.

1.6.1. Thermal analysis

Instruments designed to study the thermoanalytical properties of materials have been around since the mid-nineteenth and early twentieth centuries. Thermograms that result from these techniques supply the temperature dependencies of a material's thermodynamic properties and physicochemical reaction kinetics [28]. Since the initial development of these techniques, the dual measurement of thermogravimetric analysis and differential scanning calorimetry has been made possible so that a more thorough analysis can be performed.

Thermogravimetric analysis (TG) allows the weight of a given material to be monitored as the temperature is raised at a controlled rate. A weight gain on a thermogram is indicative of the adsorption of a volatile product in the material, while a weight loss indicates the decomposition or volatilization of the material. With differential scanning calorimetry (DSC), the change in relative heat flow (current) supplied to a sample that is required for chemical processes to occur is measured. When heat is being supplied to a sample, it can represent melting, evaporation, dehydration, or phase changes. The resulting curve on the thermogram is referred to as an endothermic peak. Exothermic peaks characterize the processes in which heat is being given off by the sample that can signify crystallization or oxidation [29]. Figure 2 demonstrates the endothermic and exothermic peaks of a sample of $CsSrBr_3$ that was synthesized at the Scintillation Materials Research Center (SMRC). The melting and crystallization temperatures were determined for the sample from this thermogram to be 758 and 738°C respectively. The combination of FT-IR spectroscopy and thermal analysis provides information about the oxygen and moisture containing impurities.

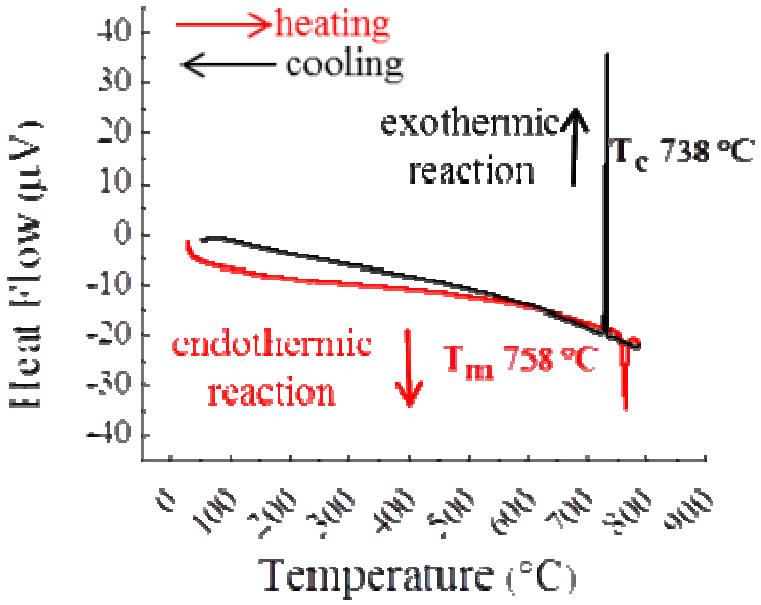

Figure 2. Example of a DSC curve from a $CsSrBr_3$ sample.

1.7 Hygroscopicity

As discussed previously, hygroscopic materials readily adsorb moisture from the atmosphere, and in the case of scintillation materials, this can provide many undesirable challenges. Hygroscopicity is a measure of how readily a material reacts with moisture. If left in regular atmospheric environments, these materials will begin to deliquesce, or change to liquid state. This poses an obvious threat the crystal quality of the scintillator, and quenches the light yield. As a means of protecting these materials so that they can be used in radiation detection applications, careful packaging measures are necessary. While the benefit of packaging is clear [30], the process is continually being refined. The packaging process requires meticulous execution, and can modify the light yield and energy resolution. Determining the hygroscopicity has historically been of a qualitative nature within the metal halide inorganic scintillator community. Often times the hygroscopicity of scintillators is briefly alluded to in literature by simply stating if a specific compound is hygroscopic or not. However, this behavior can be more concretely defined.

1.7.1. Dynamic vapor sorption

The groundwork for the instrumentation for the study of humidity related behaviors of materials was laid by a team of scientist from the University of Turku that would lead the way to developing the dynamic vapor sorption technique (DVS) [31]. In their work they disclosed an invention that was capable of monitoring the weight variation of materials in an environment with a specific temperature and humidity. The data collected by using the DVS method can be plotted into a graph that showcases the rate at which a material adsorbs moisture by determining the slope of the resulting line as seen in Figure 3 [32]. This technique is useful in not only determining the hygroscopicity of grown crystals; it can also give an idea of the degree of hygroscopicity in the raw materials used to make each compound.

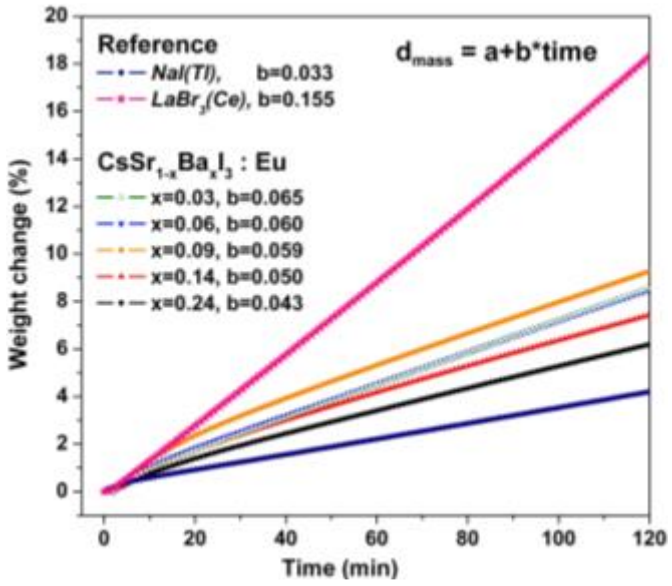

Figure 3. Example of hygroscopicity curves of $CsSrI_3$: Eu, Ba as compared with NaI: Tl and $LaBr_3$: Ce.

1.8 Development of $CsSrI_3$: Eu

The compound $CsSrI_3$: Eu was singled out as a promising candidate for further development at the SMRC. The crystal structure for $CsSrI_3$ has been previously reported as orthorhombic with a *Cmcm* space group [33]. There is no available phase diagram for $CsSrI_3$, however a phase diagram for $CsEuI_3$ is available and is a congruently melting compound. It was reasonable to assume that $CsSrI_3$ would also melt congruently as a result of the Sr^{2+} and Eu^{2+} having similar ionic radii (1.12 □ for Sr^{2+} and 1.09 □ for Eu^{2+}) and valence states. It was observed that the $CsSrI_3$ crystalized readily, and without the cleavage planes that plague other promising scintillator materials such as $LaBr_3$: Ce^{3+} [9-10].

The desirable qualities that a metal halide scintillator should have are examined. As discussed in section 1.1.1, it is desirable for a scintillator to have a density of roughly 5 $g \cdot cm^{-3}$ so that the material will have suitable stopping power and favorable economic production value. It is necessary for the wavelength of the emitted light from a scintillator

to closely match the maximum sensitivity region for the detector. Photomultiplier tubes (PMTs) that are commonly used in radiation detection devices have a sensitivity from 400-430 nm. Furthermore, it is necessary for a scintillator to have a high light yield and energy resolution. The 1" diameter $CsSrI_3$: 7% Eu grown at the SMRC can be seen in Figure 4 [9]. Table 1 compares the scintillation properties of $CsSrI_3$: 7% Eu^{2+} with recently studied Eu activated scintillators in addition to commercially available metal halide scintillators. One of the standard metal halide scintillators, NaI: Tl, is included to demonstrate benchmark scintillation characteristics.

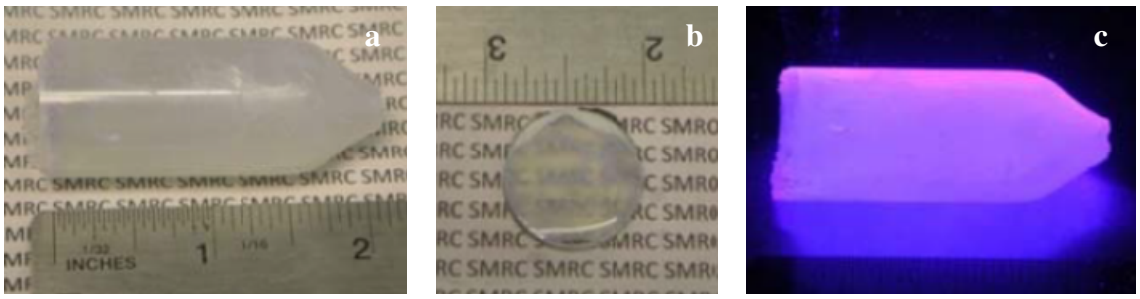

Figure 4. $CsSrI_3$: 7% Eu; a) 1" diameter, 2" long crack free boule, b) polished slab, c) boule under 255 nm UV.

Table 1. Scintillation characteristics of $CsSrI_3$: 7% Eu^{2+} as compared to other scintillators.

Scintillator	**Density (g/cm^3)**	**Light output (ph/MeV)**	**Energy resolution at 662 eV**	**Scintillation decay time (ns)**	**Emission (nm)**
SrI_2: 6% Eu [5]	4.55	115,000	2.8 %	1,200	435
$CsBa_2I_5$: 7% Eu [6]	5.00	97,000	3.8 %	48 (1%), 383 (16%), 1,500 (68%), 9,900 (15%)	435
BaClI: 5% Eu [8]	4.60	54,000	9.0 %	--	--
BaBrI: 8% Eu [13]	5.20	97,000	3.4 %	70 (1.5%), 432 (70%), 9,500 (28%)	412 (42%), 426 (58%)
$CsSrI_3$: 7% Eu [10]	4.29	73,000	3.9 %	3,200	455
$LaBr_3$: 5% Ce [37]	5.10	65,000	2.8 %	16	380
NaI: Tl [37]	3.70	39,000	6.5 %	250	415

One of the highlights of comparing $CsSrI_3$: Eu with BaClI: Eu is that it out-performs BaClI: Eu in terms of light yield and energy resolution. While, BaBrI: Eu and $CsBa_2I_5$: Eu have higher light output and marginally better energy resolution than $CsSrI_3$: Eu, the decay time of $CsSrI_3$: Eu is preferable by contrast since it is reportedly a single component versus the multiple component decay times of BaBrI: Eu and $CsBa_2I_5$: Eu.

The light output and energy resolution of SrI_2: Eu are higher than $CsSrI_3$: Eu, and this may be due to the challenging nature of synthesizing a ternary compound versus a binary compound. While the scintillation properties are quite competitive with the other Eu doped scintillators, $CsSrI_3$: Eu also demonstrates a hygroscopic behavior [9]. A deeper understanding of what causes the hygroscopic nature of $CsSrI_3$ along with the challenges provided by the presence of unintentional impurities in inorganic scintillators was desired.

1.9 Objective

The scintillator community has become concerned about the quality of raw materials used to synthesize metal halide scintillators. The presence of oxygen and/or moisture impurities within a raw material can be detrimental to the overall crystal quality of a metal halide scintillator. Given the raw materials' hygroscopic nature, the final crystal would uptake water which would lead to the degradation of the transparency of the grown boule. Additionally, oxygen and moisture impurities have been reported to cause quenching of the luminescence in scintillators. The objective of this research was to identify impurities in the raw materials, and furthermore, define parameters to purify raw materials as necessary. The experimental procedures implemented for this study have not been widely used by the scintillator community to address the concern about the quality of the raw materials for single crystal growth. The metal halide scintillator $CsSrI_3$: Eu was selected as an ideal material to use for this study based on its promise in □-ray detection applications in both the medical and homeland security fields. The primary focus of this work was to determine processing protocols for $CsSrI_3$: Eu based on the findings from a systematic experimental study of the impurities, low temperature response, and hygroscopicity of its raw materials. For the investigation of impurities present in the as-received raw materials, it was determined that optical spectroscopy and thermal analysis would be appropriate for this research. Moreover, this approach can be applied to the future development of other promising metal-halide scintillation materials.

CHAPTER 2 EXPERIMENTAL PROCEDURE

The steps taken to complete this study can be seen in figure 5. First, an investigation of the as-received raw materials to identify –OH containing impurities, followed by the determination of adequate thermal treatment. This information was used to design sample sets for rapid melt synthesis with different drying parameters. The optical and scintillation characterization of synthesized sample sets were then evaluated to determine the effectiveness of the drying procedure. Sample preparations for characterization and synthesis took place in a MBraun Unilab glovebox that maintains an atmosphere containing < 1 parts per million (ppm) of O_2 and H_2O. The starting materials CsI (99.999% purity), SrI_2 (99.995% purity), and EuI_2 (99.99% purity) were analyzed with FT-IR, DSC/TG, and DVS techniques.

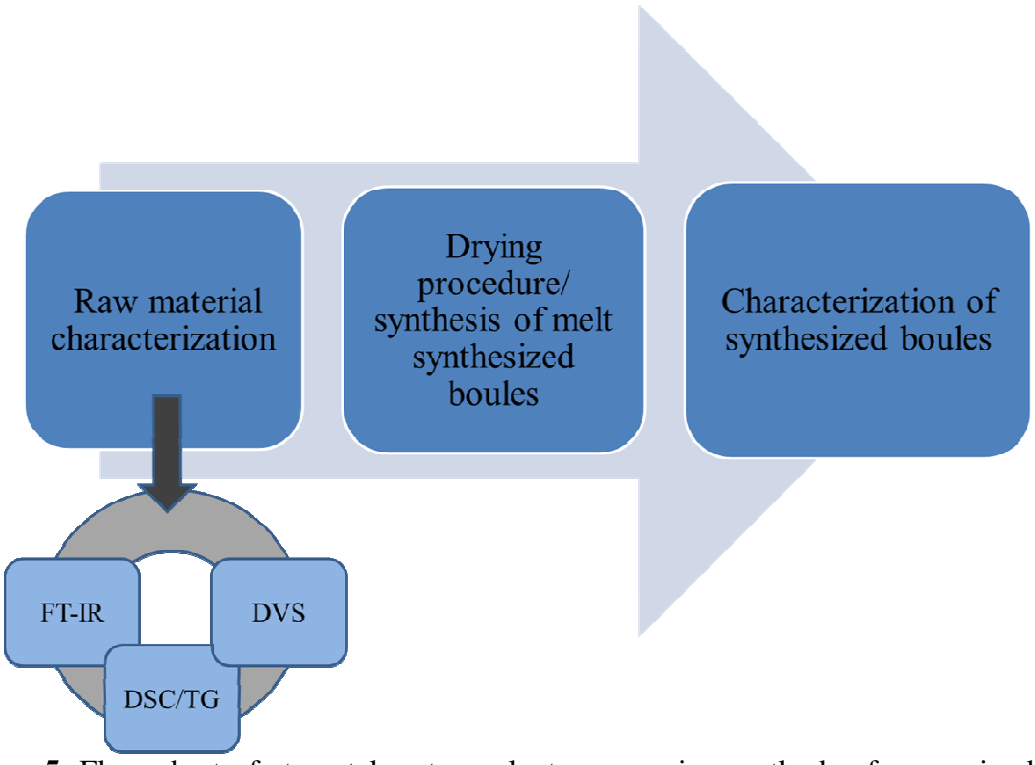

Figure 5. Flow chart of steps taken to evaluate processing methods of as-received raw materials for the synthesis of $CsSrI_3$: Eu.

2.1 Fourier transform infrared spectroscopy

Fourier transform infrared spectroscopy uses the technology of the Michelson interferometer as seen in figure 6. Light from a source is collimated and divided at a beamsplitter into two beams of equal amplitude [34]. The beams are reflected by two mirrors; one fixed, and one moving. The beams strike the beamsplitter and recombine in a direction toward the detector.

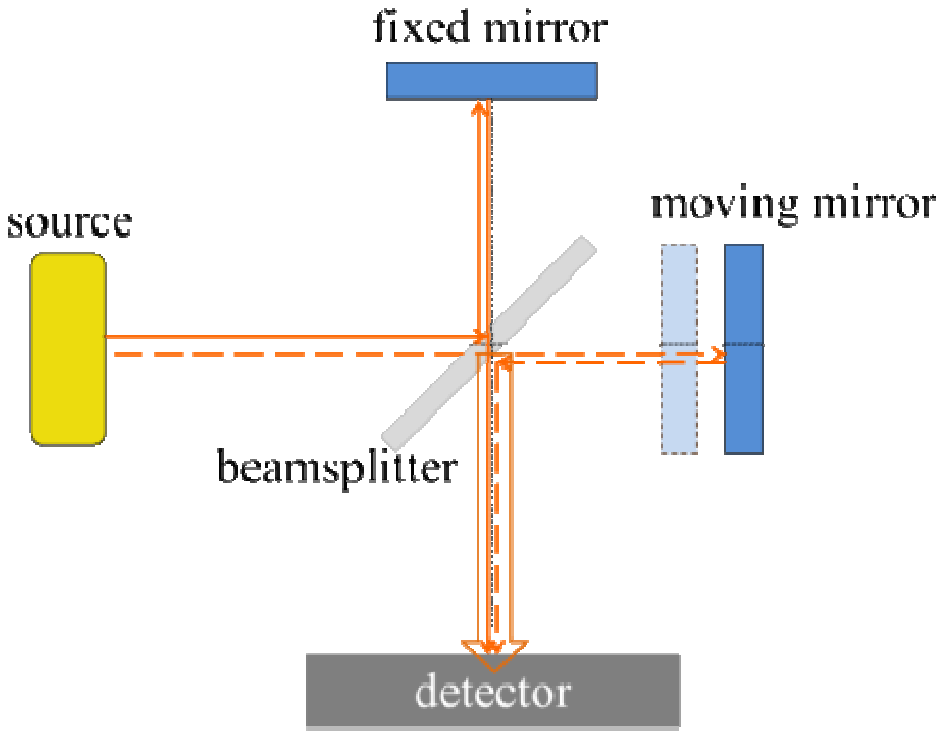

Figure 6. Sketch of Michelson interferometer.

Light that is collected at the detector produces an interferogram that is the result of the interaction of the different waves created by the separate beams coming from both mirrors. Interference occurs when multiple waves are combined in the same time and space with the same sign amplitude (constructive) or opposite sign amplitude

(destructive). A Fourier transform algorithm is applied to an interferogram to convert the information into a spectrum by converting the time-varying wave and converting it into its constituent frequencies [35]. The FT-IR technique can be used to find the linear absorption coefficient, α, which describes how much light a material absorbs, and can be defined by using the data collected from the spectrum and the relationship seen in equation 10 that modifies Beer's Law [36],

$$A(\nu)= \frac{1}{\ln 10}\ \alpha * t \quad \text{(eq. 10)}$$

where A(ν) is the absorbance at a given wavenumber in cm^{-1}, and t is the sample thickness (cm). A tungsten light source is used in FT-IR to excite molecules in a sample and create a change in the dipole moment of a molecule.

A BioRad FTS6000 spectrometer (Figure 7) was used to perform FT-IR spectroscopy on as-received starting materials. A mortar and pestle that had been dried in an oven overnight at 175°C was used to grind approximately 150 mg of as-received raw material. The resulting powder was then loaded into a bolt press and a pellet was formed. The bolt press was sealed in an air tight container while still in the glovebox, and then transferred to the spectrometer. A baseline spectrum was measured prior to transferring the sample to the spectrometer to calibrate measurements of each sample against the condition inside the spectrometer without the sample. The average of 64 scans was used working at a resolution of 4 cm^{-1} with the range of the reported spectra occurring between 4000-700 cm^{-1}. All measurements were made in transmission in an inert gas environment.

Figure 7. FTS 6000 spectrometer.

2.2 Thermal analysis

A baseline measurement of an empty Al_2O_3 crucible with a lid that was measured under a steady flow of Ar gas in the Setaram Labsys Evo DSC/TG/DTA was necessary to make proper corrections to the heat flow and thermogravimetric curves generated by the Al_2O_3 crucibles filled with raw materials. The baseline measurement for as-received raw material experiments were programmed to stabilize the furnace at 40°C for 5 minutes and then raised to 640°C at a rate of 10°C/min and then cooled back down to room temperature (RT) at the same rate. Sample weights for the raw material in bead form were 50 mg $\pm$ 5 mg. The samples were loaded into a 100 µL Al_2O_3 crucible that had been used to measure the baseline. The Al_2O_3 crucible was sealed in a jar in the glovebox before transferring to the Labsys Evo in an attempt to reduce overexposure to atmosphere prior to the measurement. All measurements were made with an empty Al_2O_3 crucible in the reference portion of the DSC rod pan so that it could be used to measure the heat flow curve of the raw material sample. Heat Flow and weight variation was recorded as a function of temperature. A baseline subtraction was performed on the curves in the Calisto Software and the resulting curves were evaluated.

2.3 Dynamic vapor sorption

The hygroscopicity of the raw materials was determined by using the dynamic vapor sorption technique with a DVS Intrinsic instrument as seen in Figure 8. The weight of materials loaded onto the sample pan was 32 $\pm$ 1 mg and once loaded, was sealed in a jar while in the glove box before being transferred to the DVS Intrinsic. The temperature was set to 25°C with a relative humidity (RH) of 40%. The DVS Intrinsic controls the RH by varying the amount of dry or wet gas from the lower portion of the instrument. The desired level of humidity is created in the sample chamber located in the center of the instrument where the sample pan is connected to a balance. The balance is located in the uppermost portion of the instrument. The sample's weight is monitored over a desired amount of time along with the temperature, and relative humidity within the sample

chamber. This information is supplied to a processor that records these values. A large slope of the resulting mass sorption curve would indicate that a material is hygroscopic.

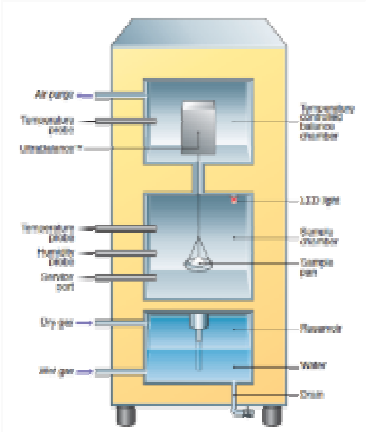

Figure 8. Diagram of the DVS Intrinsic.

2.4 Synthesis

Synthesized samples of $CsSrI_3$ with 0.01 atomic % and 7 atomic % Eu with different drying procedures were studied by analyzing scintillation characterization. Ampoules used for synthesizing and drying materials were rinsed with deionized water and subsequently acetone and then dried in an oven at 175°C. Samples of $CsSrI_3$ with 0.01% and 7% Eu were loaded into ampoules that were connected to a vacuum station. The sample was then subjected to a drying procedure while under a vacuum of between 10^{-3} and 10^{-6} torr for a period of at least 2 hours before being sealed with a H_2-O_2 torch. Different vacuum levels were used to determine the effect it had on the synthesis of $CsSrI_3$: Eu. Nine samples were created with the intention of observing the lower energy emission bands caused by oxygen in 0.01% Eu doped $CsSrI_3$. Table 2 lists the drying procedures used for these samples.

Table 2. Drying conditions for the 0.01% Eu and 7% Eu doped $CsSrI_3$.

Sample Name	Eu %	Sample Weight	Drying Temperature	Drying/ Evauation Time (hours)	Vacuum level at time of seal
All dried	0.01	10 g	225°C	8	$7 * 10^{-6}$
SrI_2 & EuI_2 dried	0.01	10 g	1st step 225°C 2nd step ---	8 8	$5 * 10^{-6}$ $6 * 10^{-6}$
Non-dried	0.01	10 g	---	9	$9 * 10^{-6}$
All dried	7	10 g	225°C	8	$5 * 10^{-6}$
Non-dried	7	10 g	---	9	$8 * 10^{-6}$
All dried	0.01	5 g	225°C	8	10^{-3}
SrI_2 & EuI_2 dried	0.01	5 g	1st step 225°C 2nd step ---	8 8	10^{-3}
Non-dried	0.01	5 g	---	9	10^{-3}
All dried	7	5 g	225°C	8	10^{-3}
Non-dried	7	5 g	---	9	10^{-3}
All dried	0.01	5 g	225°C	2	$2 * 10^{-6}$
SrI_2 & EuI_2 dried	0.01	5 g	1st step 225°C 2nd step ---	2 3	$2* 10^{-6}$ $2 * 10^{-6}$
Non-dried	0.01	5 g	---	3	$2 * 10^{-6}$
All dried	7	5 g	225°C	2	$2 * 10^{-6}$
Non-dried	7	5 g	---	3	$3 * 10^{-6}$

One sample was created by drying a mixture of CsI, SrI_2, and EuI_2 at 225°C for at least 2 hours while under evacuation, hereafter referred to as all dried. Other samples annotated as the SrI_2/EuI_2 dried series employed drying of the SrI_2 and EuI_2 at 225°C for at least 2 hours while under evacuation. The dried raw materials were then mixed with CsI and loaded into another ampoule that was held under vacuum for 3 hours. The last sample set, the non-dried series, was not dried, but was evacuated for a minimum of 3 hours. All ampoules were sealed with a vacuum in the range of 10^{-3}- 10^{-6} torr. The six 7% Eu doped $CsSrI_3$ samples were dried with the similar conditions as the 0.01% Eu doped $CsSrI_3$ samples. The purpose of the synthesis of the $CsSrI_3$: 7% Eu was to observe the effects of the drying parameters on the light output and energy resolution of the resulting boules.

A differential scanning calorimetry measurement had been performed on $CsSrI_3$: 7% Eu during the initial development of the material and it was determined that it had a melting temperature of ~645°C [9].The samples were ultimately synthesized by soaking the material in a clamshell furnace at a temperature that was slightly higher than previously reported melting temperature for at least 3 hours and then cooling the material to room temperature over a period of at least 2 hours. The heating and cooling process had to be repeated multiple times in combination with reorienting the ampoule vertically within the furnace to promote thorough mixing. The sample set was divided by the Eu concentration such that all samples with the same concentration experienced the same thermal treatment (i.e. all 0.01% Eu doped samples that had been dried for the same amount of time and under approximately the same vacuum level went into the same furnace at the same time). Further discussion of precise synthesis conditions are provided in the next chapter.

2.5 Luminescence and scintillation characterization

The synthesized samples were evaluated with characterization techniques to determine how impurities affect the scintillation and optical properties. The samples were prepared in a glove box and were cut into cubes with varying dimensions that will be detailed in the next chapter. Dimensions of specific sample sets will be described in the following chapter. Samples were placed in a jar with paraffin oil inside the glovebox that was then transferred to instruments outside of the glovebox.

Radioluminescence spectra were measured at room temperature. A CMX-003 X-ray generator tube that was operated at a voltage of 35 kV and a current of 0.1 mA was used to irradiate the sample with x-rays. The samples were measured in reflection mode geometry at a rate of 200 nm/min. The spectra were recorded from 200 to 800 nm by the ACTON 2150i spectrometer.

Pulse height spectra were measured with a Hamamatsu 3317-50 photomultiplier tube (PMT). Three 10 microcurie (μCi) ^{137}Cs sources were used to irradiate the samples with 662 keV □-rays. A Spectralon reflector cap was used to reflect the light onto the

PMT. A Canberra 2005 pre-amplifier, Ortec 672 amplifier with a shaping time of 10 μs, and a Tukan 8k multi-channel analyzer was used in conjunction with the PMT to create the pulse height spectra.

CHAPTER 3 Experimental Results and discussion

Results from the raw-material characterization were used to identify optimal drying conditions to enable successful synthesis of $CsSrI_3$: Eu. The optical and scintillation properties of the samples produced with different drying conditions were compared to analyze the veracity of the hypothesis stipulated by the raw-material characterization that will be discussed further.

3.1 Fourier transform infrared spectroscopy

The raw materials that are used to synthesize $CsSrI_3$: Eu were characterized with FT-IR in an attempt to identify possible contaminants included within the as-received materials.

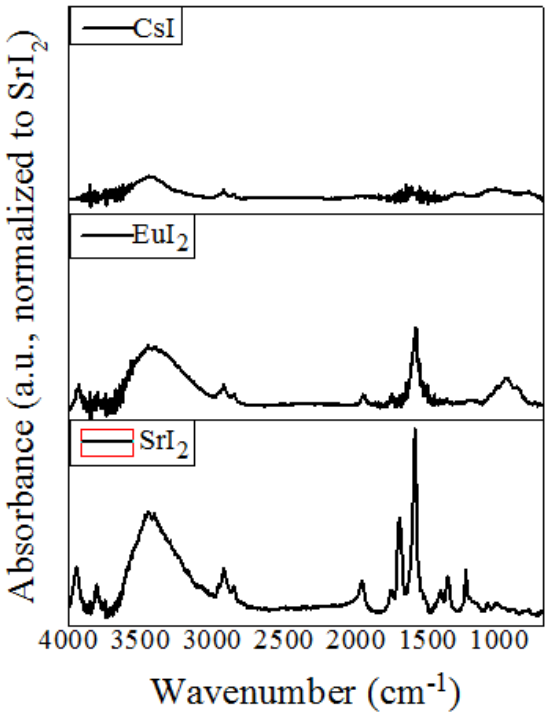

Figure 9. IR spectra of as-received CsI, SrI_2, and EuI_2 normalized to the SrI_2 spectra.

Figure 9 demonstrates the presence of oxygen and/or moisture impurities in all of the raw materials used in the synthesis of $CsSrI_3$: Eu. Since the measurement was made in transmission mode, the resulting spectra is a representation of the bulk material, as opposed to other infrared techniques, such as attenuated total reflectance, that only measures the surface of the materials. All starting materials have a peak in the wavelength range 3550-3200 cm^{-1} (OH stretching), although it should be noted that the intensity of this peak for CsI is far less than that of EuI_2 and SrI_2. The starting materials also appear to exhibit two peaks in the 2950-2840 cm^{-1} that can be attributed to a C-H bond. Both SrI_2 and EuI_2 have a peak present between 1630-1600 cm^{-1} (HOH bending), which is commonly attributed to the presence of moisture. The information collected from the TG/DSC measurements follow this same trend.

3.2 Thermal Analysis

Thermal analysis techniques were pursued to identify temperatures at which possible thermal processes took place. There are no observable reactions that occur in the heat flow and TG curves of CsI raw materials as seen in Figure 10. This observation correlates with the IR spectra of as-received CsI given the absence of the HOH bending peak in the IR spectra. In the event that the HOH bending peak was observed in the IR spectra, it would be reasonable to expect to see a dehydration occuring below the melting temperature of the sample, as is the case with both SrI_2 and EuI_2.

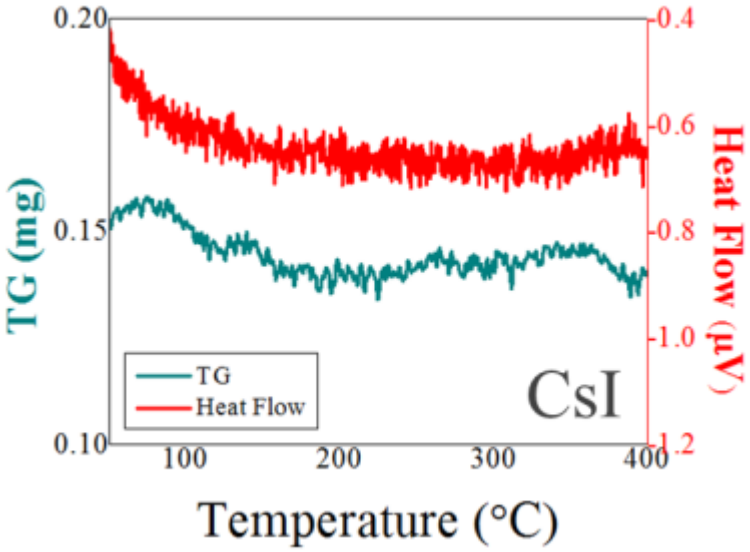

Figure 10. Heat flow and TG curves of as-received CsI.

The heat flow and TG curves of SrI_2 seen in Figure 11 shows an initial mass loss of between 50-100°C followed by an absorption between 100-170°C. Where an endothermic peak begins at 179°C in the heat flow curve, there is also a coinciding mass loss observed in the TG curve. The mass loss and endothermic reaction both end at approximately 225°C. This observation has been reported for SrI_2 raw materials and SrI_2 hydrate phases ($SrI_2 \cdot xH_2O$) that show a similar process of dehydration appearing at a

similar temperature [39, 40]. Recommended treatment of this material would be to dry the material at a temperature ~ 225°C.

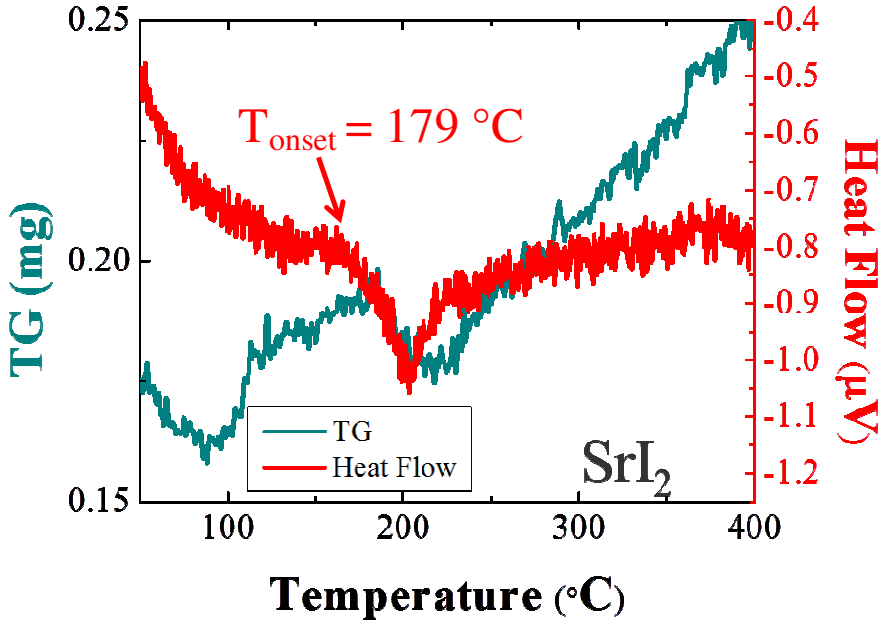

Figure 11. Heat Flow and TG curves of as-received SrI_2.

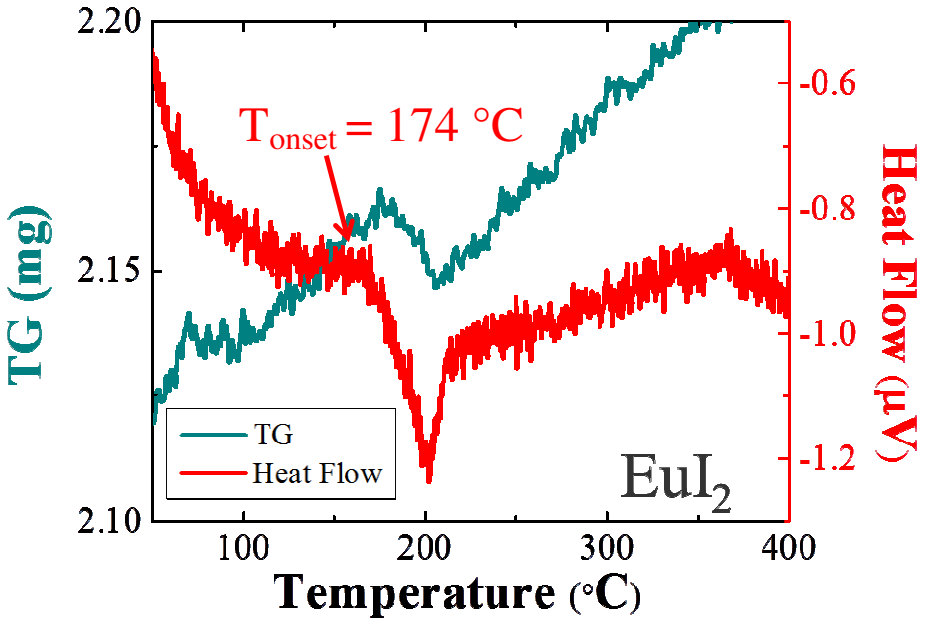

Figure 12. Heat Flow and TG curve of as-received EuI_2.

Heat flow and TG curves for EuI_2 are displayed in Figure 12. The TG curve shows a weight variation that has corresponding endothermic process occuring 174°C. Presumably, the Eu hydrate that is present in very low concentration in the as-received raw material is dehydrating between 174-210°C, which is similar to what has been reported [40]. A temperature of ~225°C is likewise appropriate for drying this material.

A drying procedure for processing the as-received materials was formatted based on the results from the thermal analysis results. Since CsI does not appear to have any evaporation occurring at pre-melting temperatures, it follows that it would not necessarily require any drying procedure. However, both SrI_2 and EuI_2 demonstrate a need to be heated to a temperature ~225°C before being used to synthesize $CsSrI_3$: Eu to dehydrate the material and prevent possible oxyhalide formation or other modes of decomposing the sample.

3.3 Dynamic vapor sorption

Hygroscopicity of the raw materials was determined by using DVS. The hygroscopicity curves for the starting materials are found in Figure 13. The horizontal curve of the CsI samples indicates that there is no moisture sorption that occurs for this raw material. The slope (m) of the moisture sorption curves of EuI_2 and SrI_2 indicates that these raw materials are hygroscopic. The moisture sorption rate, or the measure of hygroscopicity, from lowest to highest for materials measured in this study are CsI, EuI_2, and SrI_2. The IR spectra of the starting materials reflect the trend that is noted in the hygroscopicity curve, in which the highest absorption peak of the HOH bending is present in the SrI_2 spectrum, followed by a lower intensity in the EuI_2 spectrum, and an absence in the CsI spectrum.

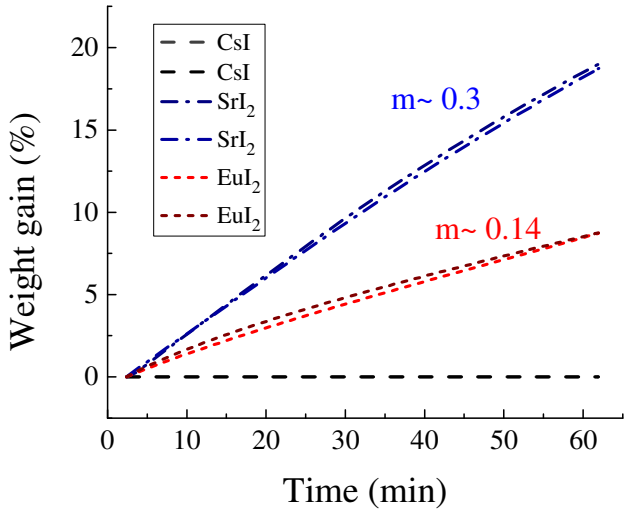

Figure 13. Moisture sorption curves of as-received CsI, SrI_2, and EuI_2.

All of the measurement techniques used to characterize these raw-materials shows good agreement with the other results presented in this work. Provided a material has a low moisture uptake rate, as is the case of the CsI raw material measured in this work, one should expect an absence of an HOH bending peak in the IR spectra along with no notable chemical reactions occurring in the TG/DSC curves prior to the melting temperature of the sample. On the other hand, if a sample is hygroscopic like EuI_2 and SrI_2, one chould expect to observe an HOH bending peak in the IR spectra along with an observable dehydration in the TG/DSC curves.

3.4 Synthesis and characterization of $CsSrI_3$: Eu boules

3.4.1 Synthesis of $CsSrI_3$: 0.01% Eu

The drying parameters of the samples created for testing the effects of drying on the scintillation properties were based on the observations from the raw-material characterization. The 0.01% Eu doped samples were created with the intention of

observing oxygen related defects in the radioluminescence spectra. As mentioned in the introduction, the oxygen defect luminescence in BaBrCl: Eu have been noted to create a tail that occurs at a longer wavelength than the Eu emission band [18-19]. The concentration of Eu in the sample has to be low enough so that the emission band of the oxygen related defect does not get suppressed.

Initial synthesis of the samples that had been dried and/or evacuated to a pressure of 10^{-6} torr for at least 8 hours took place in a 24 zone Mellen furnace in which all zones were initially raised to 625°C. The hot zone was programmed to be heated to 660°C and was moved through the charge one zone at a time. After the entire furnace had been raised to 660°C and soaked for 5 hours, the furnace was cooled to room temperature over 18 hours. Initial synthesis of the samples that had been dried and/or evacuated to a pressure of 10^{-3} torr for at least 8 hours took place in a clamshell furnace in which all three (all dried, SrI_2/EuI_2 dried, and non-dried) samples were synthesized at the same time. Likewise, all three samples that had been dried and/or evacuated to a pressure of 10^{-6} torr for at least 2 hours were synthesized at the same time. The samples were heated to a temperature of ~650°C and soaked for 3 hours and then cooled to RT over 2 hours. The results from this initial synthesis can be seen in Figure 14.

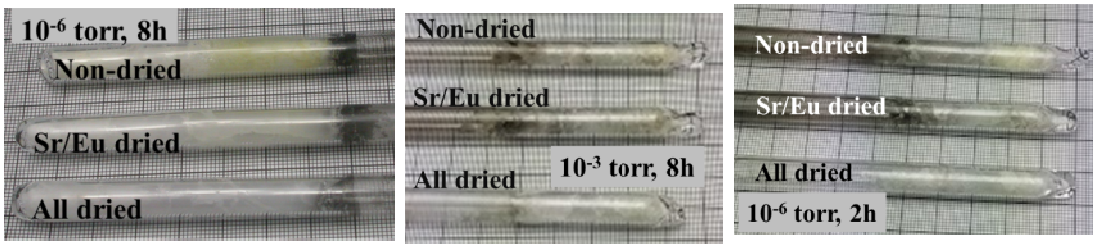

Figure 14. Samples of $CsSrI_3$: 0.01% Eu after the first synthesis cycle.

The quality of these samples within each sample set varied significantly after initial synthesis. The boules synthesized with all dried raw materials appeared to be the highest quality samples out of their sample sets. Slight discoloration of the upper portion of the boule occurred for the boule synthesized with SrI_2 and EuI_2 dried raw materials

under 10^{-6} torr for 8h. The other SrI/Eu dried boules were slightly discolored as well. It was assumed that by having a two-step drying procedure that involved separately drying the SrI_2 and EuI_2 in one ampoule, and then combining the dried material with the CsI in another ampoule provided a potential for inadvertently re-exposing the materials. The boule synthesized with non-dried raw materials under 10^{-6} torr for 8h was more opaque than the other samples and was discolored in the top portion of the 6 mm boule, additionally; this sample appeared to have more cracks than the samples that had materials that had been partially or completely dried. The samples that had been synthesized with non-dried materials and SrI_2 and EuI_2 dried materials also seemed to have more black contaminant that surrounds the top layer of the boule in comparison to materials synthesized with all dried materials. This could be because the H_2O that is observed in the FT-IR spectra and is present in the raw materials have an opportunity to react with the C-H contamination in the raw material.

In the subsequent synthesis cycles, the boules that were synthesized with materials that had experienced a drying and/or evacuation of 10^{-6} torr for 8 h were in a clamshell furnace. The samples were heated to a temperature of ~665°C for 8 hours and then cooled to room temperature over a period of 6 hours. The other samples followed the same heating and cooling parameters that they experienced in the first synthesis step. The visual observations of the samples synthesized with materials that had experienced a drying and/or evacuation of 10^{-6} torr for 8 h after the second synthesis cycle continued to indicate that the sample that was synthesized with dried materials was more transparent than the other two samples in that sample set, as can be seen in Figure 15. One of the possible explanations for the drastic change in appearance from the first synthesis step and this subsequent synthesis step is that the charges had experienced more thorough mixing as a result of having their orientation changed. The discoloration in SrI_2/EuI_2 dried and non-dried samples after the initial synthesis in the Mellen furnace could have been due to poor melting of the EuI_2.

Although the boules that had materials that had either been dried and/or evacuated to a pressure of 10^{-3} torr for at least 8 hours or 10^{-6} torr for at least 2 hours were rotated in a vertical direction, only the samples that had been synthesized with all dried materials

were able to partially flow out of their original position. The partially dried and non-dried materials did not flow out of their original position, but did appear to have mixed more thoroughly than in the previous synthesis cycle.

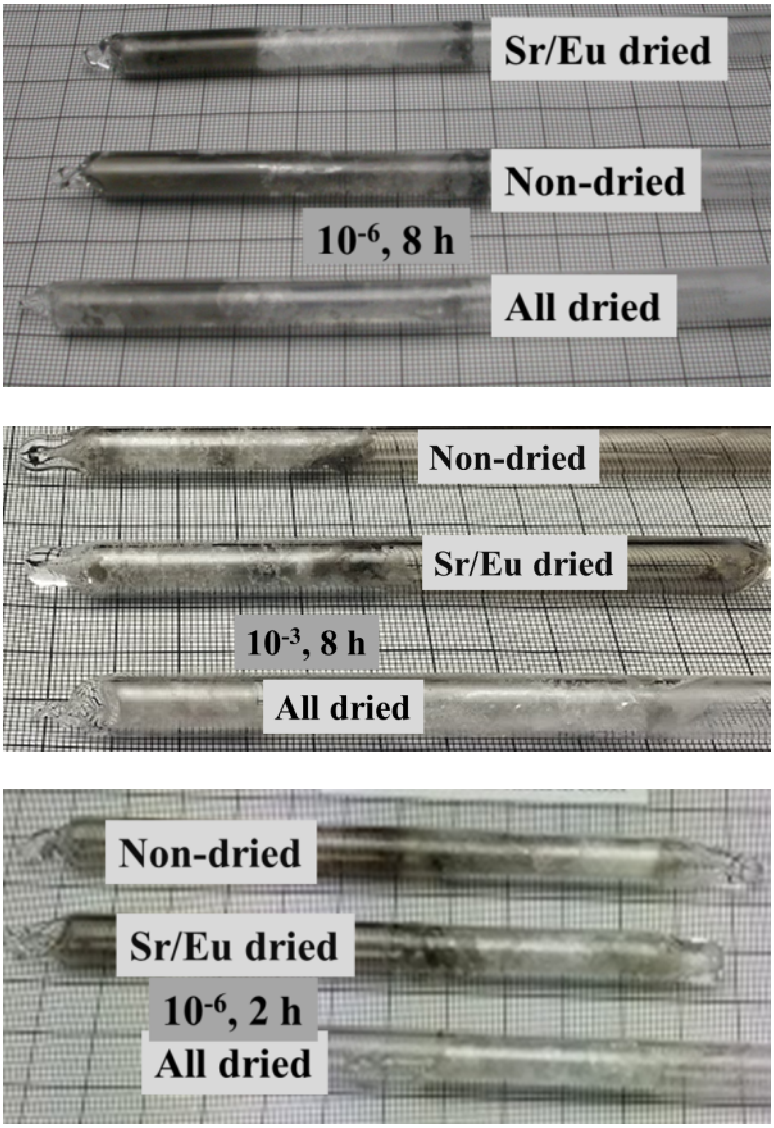

Figure 15. Samples of $CsSrI_3$: 0.01% Eu after the second synthesis cycle.

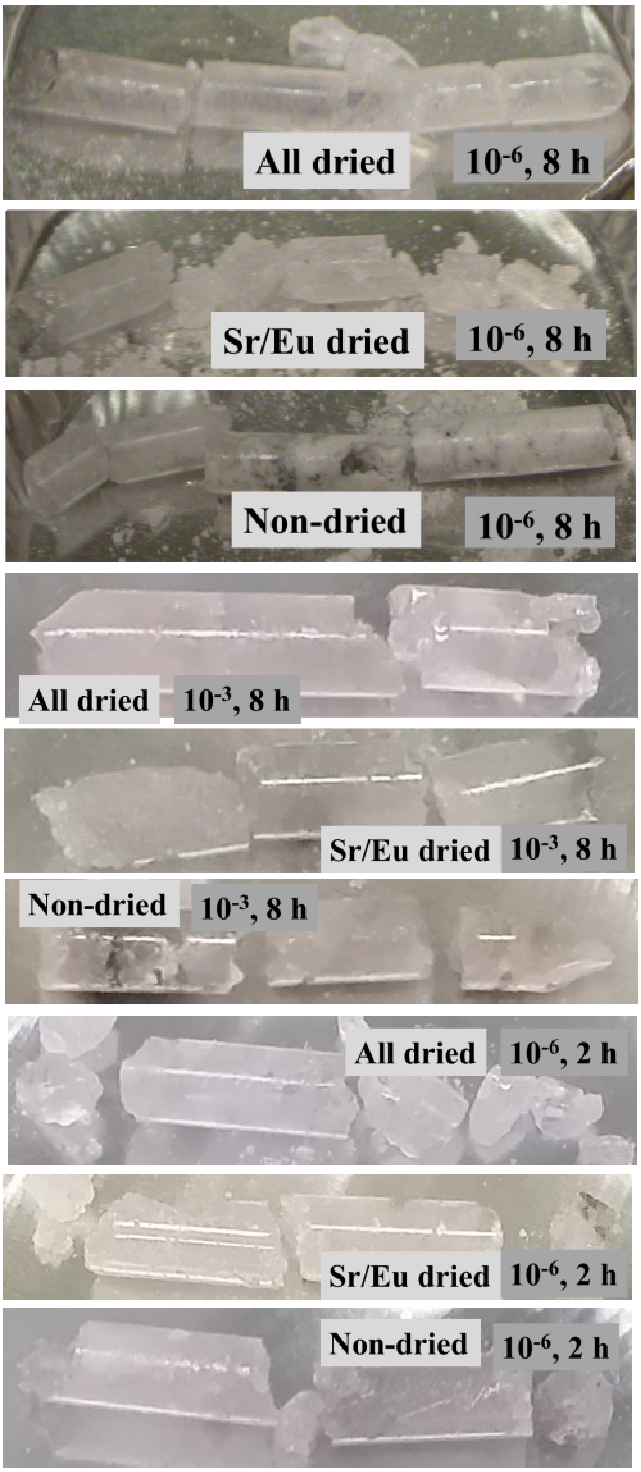

Figure 16. Samples of $CsSrI_3$: 0.01% Eu after the third synthesis cycle.

The visual comparison after the third synthesis cycle is seen in Figure 16. The boule that had been prepared with materials that had been dried and evacuated to a pressure of 10^{-6} torr for 8 hours produced the most transparent, crack-free boule. All of the boules prepared with dried materials were the most transparent out of their sample sets, and had no black particulate contamination. The SrI_2/EuI_2 dried and non-dried samples that had been dried or evacuated to a pressure of 10^{-6} torr for at least 8 hours appeared to have a translucent portion, and an opaque portion, with the boule synthesized with SrI_2/EuI_2 dried raw materials containing a smaller amount of opaque sample. The other SrI_2/EuI_2 dried samples did appear to have minimal carbon contamination at the top of the boule, while the top portion of the non-dried samples appeared to be more translucent than the lower portion of their respective boules.

3.4.1.1 Radioluminescence of $CsSrI_3$: 0.01% Eu

Samples used for radioluminescence measurements came from the lower portion of each boule so that the opaque samples would not be used for comparison. It is likely that deleterious reactions occurred in the opaque portions of boules, and so an effort was made to only compare samples that were the closest in visual quality. The dimensions of samples prepared from boules that had synthesized with materials that had been dried and/or evacuated to a pressure of 10^{-6} torr for at least 8 hours were kept at 5x4x3 mm^3. The spectra were fit with multiple Gaussian functions (where applicable) to identify the centroids as seen in figure 17. A single emission peak is observed in the dried sample that occurs at 438 nm. The emission peaks occur at 435 nm for the SrI_2/EuI_2 dried sample, and 442 nm for the non-dried sample. Tails that occur at longer wavelengths than the Eu emission peak are observable in both the SrI_2/EuI_2 dried and non-dried samples. The presence of the tail in the radioluminescence spectra of the other two samples could be indicative of oxygen related defects. It should be noted that attempts were made to measure the pulse height spectra of these samples, although, no discernible photopeak was identified in any of these samples.

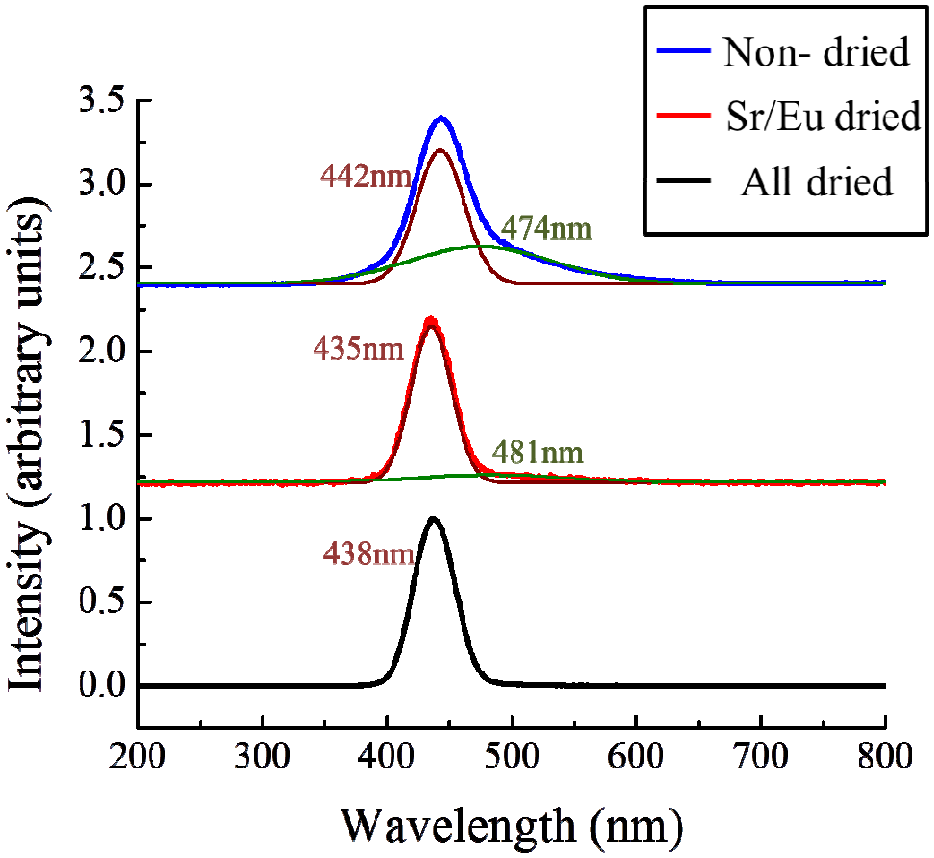

Figure 17. Radioluminescence spectra with Gaussian fitting of samples from boules that had been synthesized with materials that had been dried and/or evacuated to a pressure of 10^{-6} torr for at least 8 hours.

The dimensions of the measured samples were kept at 4x3x3 mm^3 for all of the other samples. The spectra were fit with multiple Gaussian functions (where applicable) to identify the centroids as seen in figures 18 and 19. There were no tails observed in the samples that had been dried or evacuated to a pressure of 10^{-3} torr for 8 hours and the emission peaks ranged from 440-444 nm. Meanwhile samples that had synthesized with materials that had been dried and/or evacuated to a pressure of 10^{-6} torr for 3 hours had peaks occurring between 432-433 nm, and only the non-dried sample exhibited a tail at a longer wavelength than the emission peak.

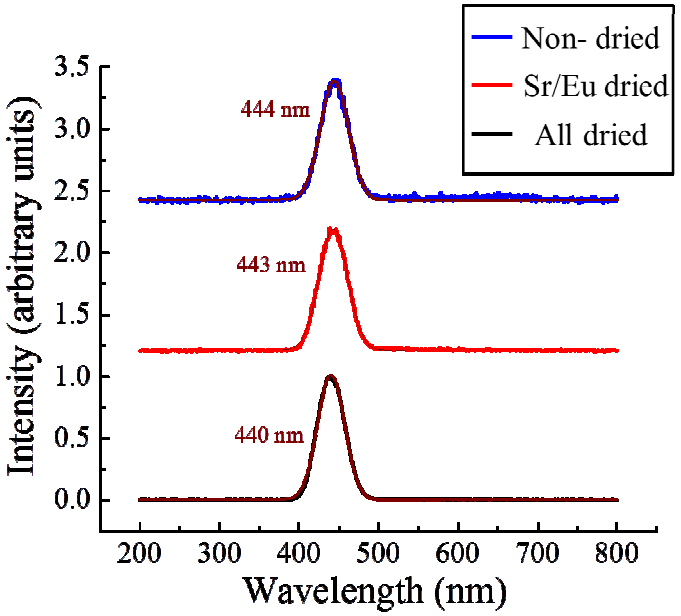

Figure 18. Radioluminescence spectra with Gaussian fitting of samples from boules that had been synthesized with materials that had been dried and/or evacuated to a pressure of 10^{-3} torr for at least 8 hours.

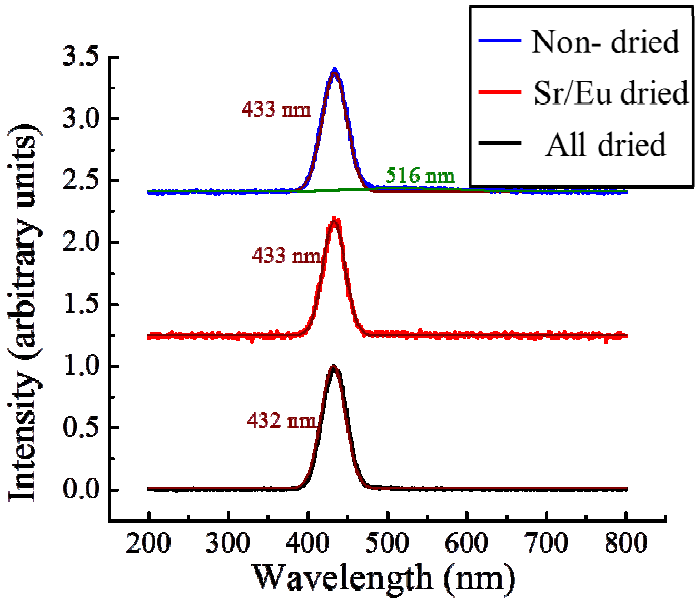

Figure 19. Radioluminescence spectra with Gaussian fitting of samples from boules that had been synthesized with materials that had been dried and/or evacuated to a pressure of 10^{-6} torr for at least 2 hours.

3.4.2 Synthesis of $CsSrI_3$: 7% Eu

Six samples were synthesized with the intention of comparing the light output and energy resolution of $CsSrI_3$: 7% Eu with different drying procedures. The result of the initial synthesis of the SrI_2/EuI_2 dried 0.01% Eu doped $CsSrI_3$ formed the design of these sample sets. The conclusion that was made after the initial synthesis of the SrI_2/EuI_2 dried samples indicated that a two ampoule drying procedure would not be beneficial, and so the SrI_2/EuI_2 dried sample was eliminated from these sample sets. Some samples were synthesized with dried starting materials (all dried) with the same drying procedure previously described in table 2 in section 2.4, while the other samples were evacuated for the same amount of time as the dried samples, but did not receive a heating treatment (non-dried). The samples that had been dried or evacuated in the small clamshell furnace for at least 8 hours all had inner diameters of 5 mm. Likewise, the samples that had been dried or evacuated in the large clamshell furnace for at least 2 hours had inner diameters of 5 mm. for The synthesis cycles that were employed in the clamshell furnace followed the same parameters described for the synthesis cycles of 0.01% Eu doped $CsSrI_3$. All ampoules pulled a vacuum on the order of 10^{-3}- 10^{-6} torr prior to sealing.

The visual observations from the initial synthesis of the $CsSrI_3$: 7% Eu indicated more contamination in the top portion of the quartz ampoules occurred in the non-dried boules as seen in Figure 20. All samples appeared to be opaque after the initial synthesis.

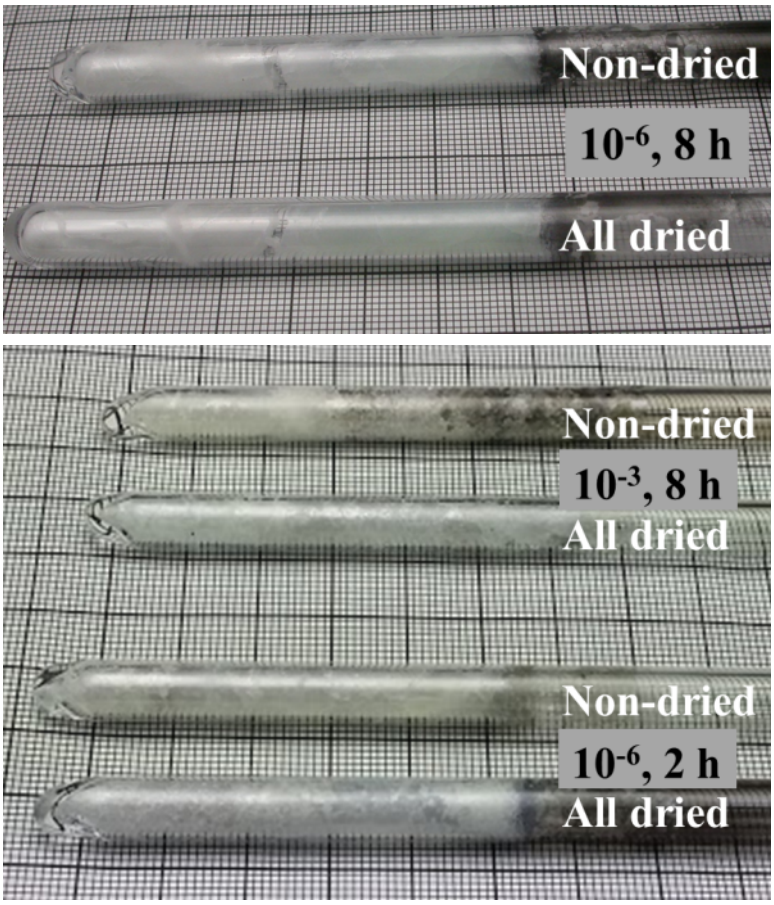

Figure 20. Samples of $CsSrI_3$: 7% Eu after the first synthesis cycle.

After the second synthesis cycle in the clamshell furnace, all boules appeared to have mixed more thoroughly and were translucent as seen in Figure 21. It should be noted that the boules that had been dried and/or evacuated to a pressure of 10^{-3} torr for at least 8 hours or dried and/or evacuated to a pressure of 10^{-6} torr for at least 2 hours were appeared to have the same issue as the 0.01% Eu doped counterparts, as is evidenced by the charges not translating through the ampoule even though the ampoules had been re-oriented vertically before heating to approximately 650°C.

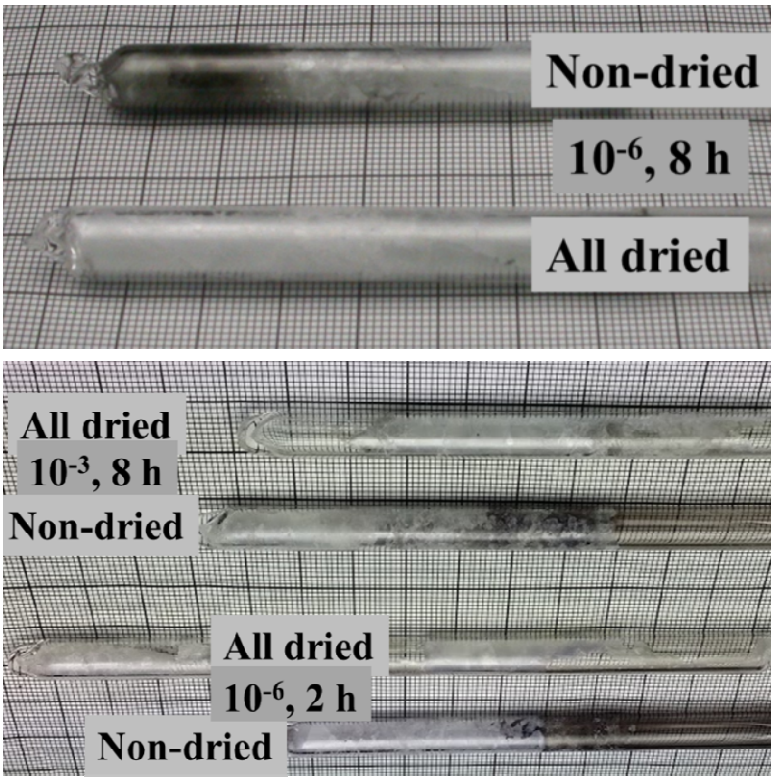

Figure 21. Samples of $CsSrI_3$: 7% Eu after the second synthesis cycle in the clamshell furnace.

Visual observations after the third synthesis cycle in the clamshell furnace provided the most dramatic differences between the samples that had been synthesized with materials that had been dried and/or evacuated to a pressure of 10^{-6} torr for at least 8 hours. The non-dried boule was completely opaque, while the all dried boule appeared to be translucent as presented in Figure 22. A Tesla coil was used to test the non-dried boule's ampoule to check for a breach, but that did not appear to have occurred. All of the boules synthesized with the dried materials had less of the black contaminant on the surface of the boule than the boules synthesized with the non-dried materials. The sample that had been synthesized with the non-dried raw materials that had been evacuated to a pressure of 10^{-3} torr for 8 hours appeared to have significant contamination on the upper portion of the boule.

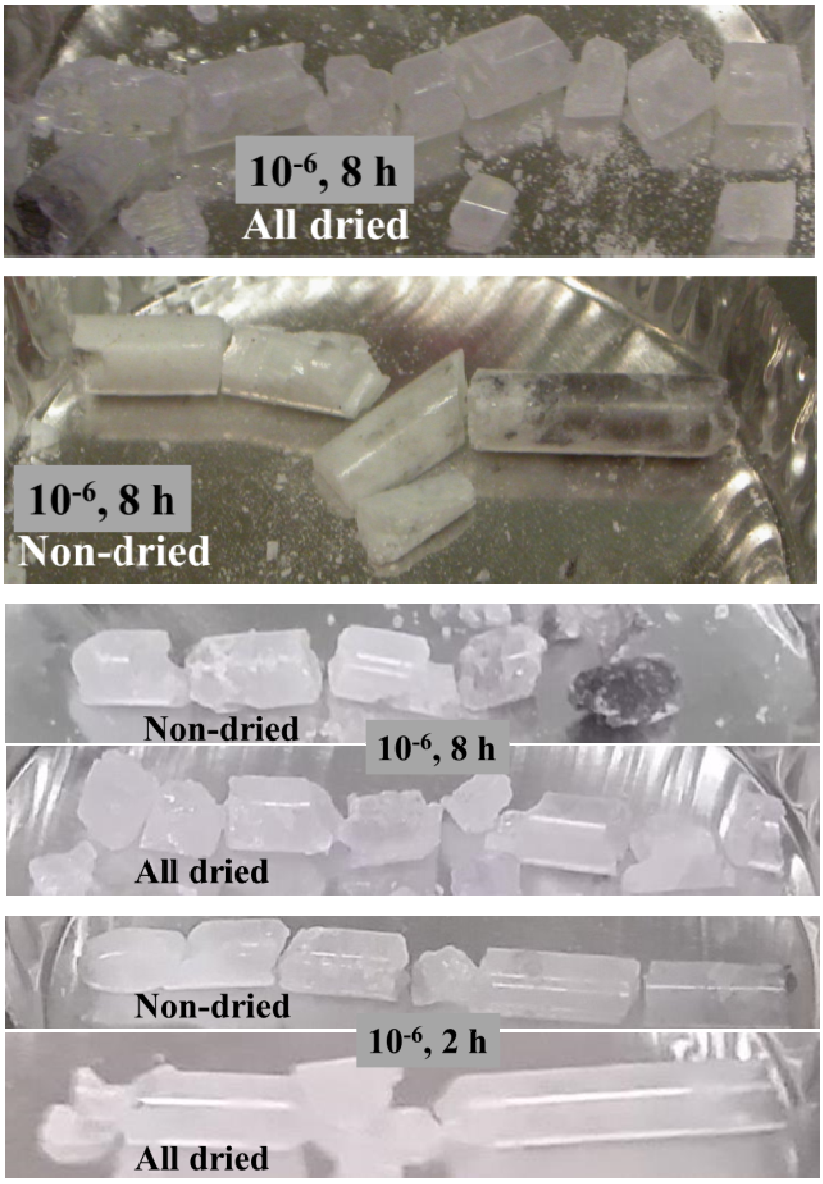

Figure 22. Samples of $CsSrI_3$: 7% Eu after the third synthesis cycle.

3.4.2.1 Pulse height spectra and radioluminescence of $CsSrI_3$: 7% Eu

The pulse height and radioluminescence spectra of these samples were recorded. Sample dimensions of the measured materials 7% Eu doped boules were kept at 3x3x5 mm^3. The samples that had been synthesized with dried raw materials did produce a measurable photopeaks. Figure 23 displays the pulse height spectra of all of the $CsSrI_3$: 7% Eu. The photopeaks were fit with a Gaussian functions to determine the centroid and

full width at half maximum (FWHM). The energy resolution can be expressed by using equation 11.

$$R = \frac{FWHM}{centroid} * 100 \text{ (eq. 11)}$$

By using the relationship described above, it was determined that the sample measured that had been synthesized with materials that had been dried and/or evacuated to a pressure of 10^{-6} for at least 8 hours had the best energy resolution as compared to all other samples prepared for the project and was 6.7%. The energy resolution from the the sample that was synthesized with materials that was dried and evacuated to a pressure of 10^{-3} torr for 8 hours is approximately 9.6 %. It should be noted that the sample that had been dried and evacuated to a pressure of 10^{-6} torr for only 2 hours exhibited an energy resolution of ~ 18%. By comparing this result to the boule that had been dried for 8 hours at a comparable vacuum level, one could argue that longer drying times will help preserve energy resolution for this particular compound.

As expected based on the visual observations of the opaque sample, there was no photopeak observed in the non-dried sample that was synthesized with materials that had been evacuated to a pressure of 10^{-6} torr for 9 hours un-dried materials seen in figure 23. The pulse height spectra of all of the other samples synthesized with non-dried raw materials, exhibited energy resolutions that were greater than 20%.

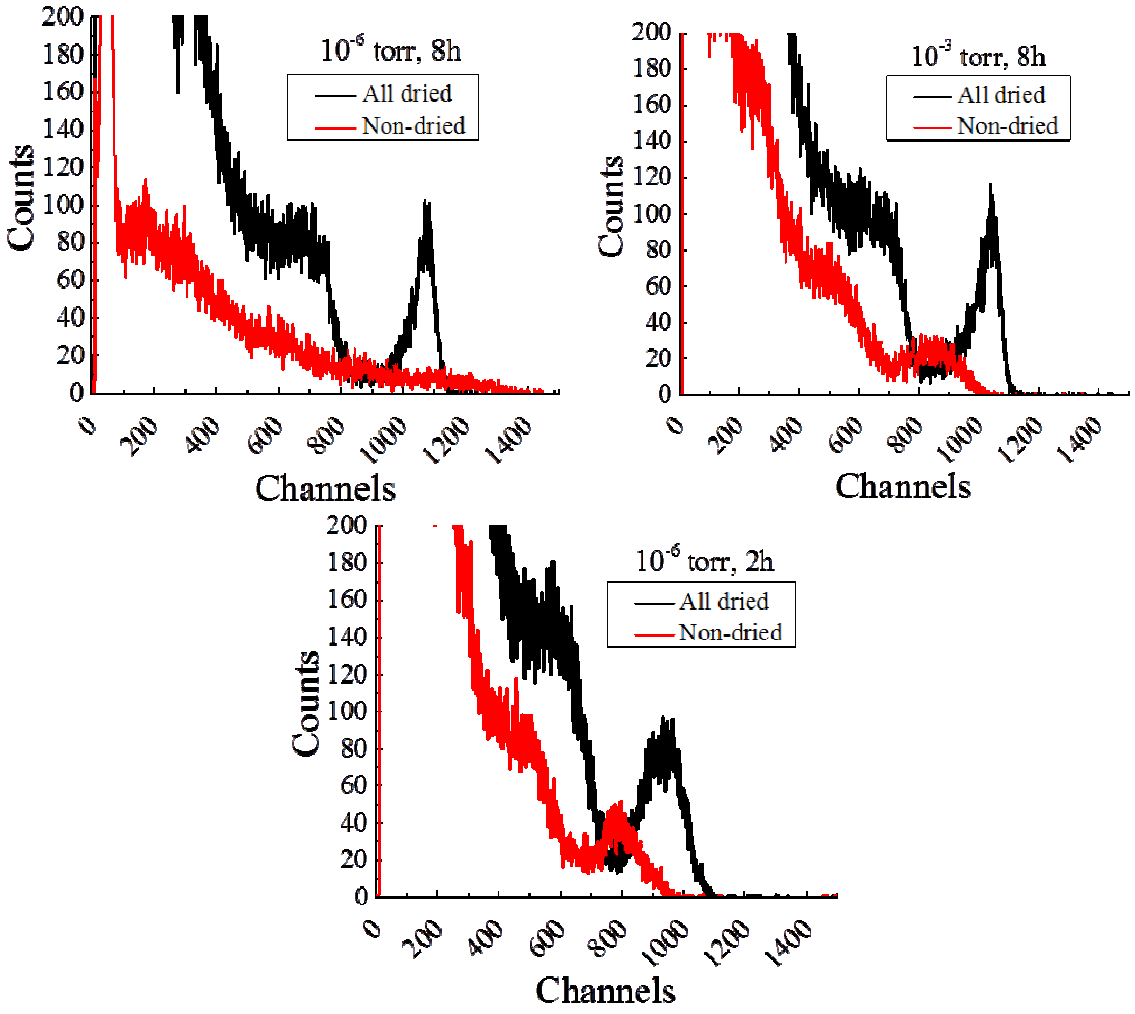

Figure 23. Pulse height spectra of the $CsSrI_3$: 7% Eu samples.

The radioluminescence was measured so that the wavelength of the emission of the X-ray excited sample could be determined. It is preferable to have a scintillator that emits light at a wavelength that is close to the wavelength of maximum sensitivity of a PMT that will be used for the detection of the scintillation light. The radioluminescence spectra for the samples synthesized with dried and un-dried raw materials can be found in figure 24 where the emission peaks occurring in a range from 451- 457 nm, which is close to the previously reported emission band at 455 nm for the 7% Eu doped $CsSrI_3$ sample [10].

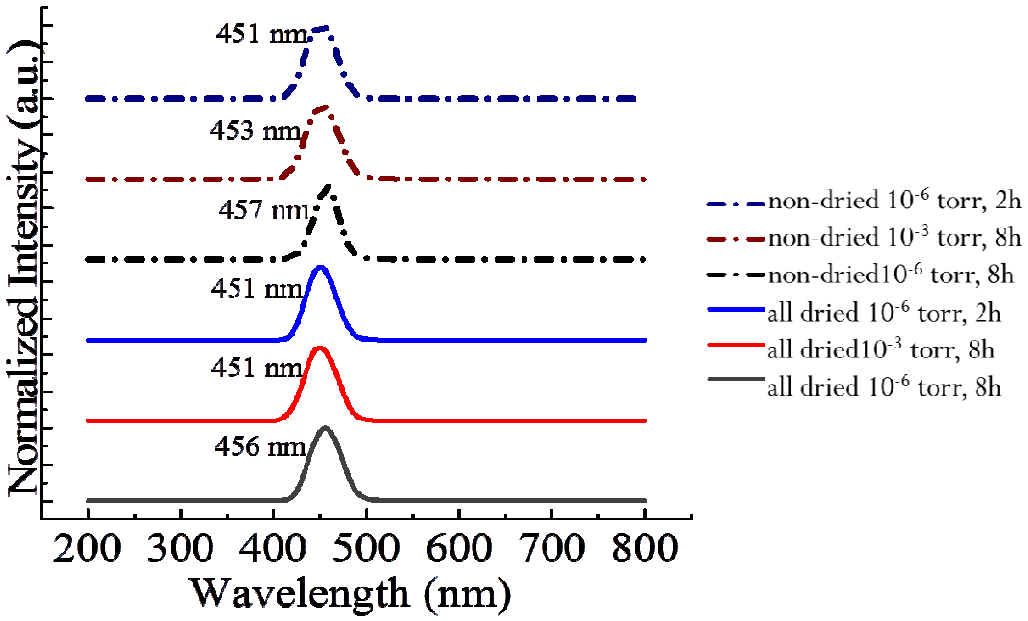

Figure 24. Radioluminescence spectra of samples of $CsSrI_3$: 7% Eu that were synthesized with dried or un-dried raw materials.

Radioluminescence is also used to determine the quantum efficiency (QE) that is dependent on the scintillation light, and can be calculated by combining the QE of the PMT and the radioluminescence spectrum of the sample. The QE is used in the estimation of the absolute light output. The absolute light output of the samples measured can be found in table 3.

Table 3. Scintillation light output and energy resolution of $CsSrI_3$: 7% Eu synthesized with different drying procedures.

All dried	Light output (ph/MeV)	Energy resolution (%)	Non-dried	Light output (ph/MeV)	Energy resolution (%)
10^{-6} torr, 8 h	54,000	6.7	10^{-6} torr, 8 h	--------	-------
10^{-3} torr, 8 h	50,000	9.6	10^{-3} torr, 8 h	40,000	~41
10^{-6} torr, 2 h	46,000	18.2	10^{-6} torr, 2 h	39,000	23.3

The best absolute light output (54,000 ph/MeV) as determined by the pulse height and radioluminescence spectra occurred in the sample that had been synthesized with the dried raw materials and had been held under evacuation at a pressure on the order of 10^{-6} torr for at least 8 hours. The energy resolution and light output for $CsSrI_3$: 7% Eu sample that was initially reported was 3.9% and 73,000 ph/MeV [10]. This could be an indication of less successful drying procedures, or it could be symptomatic of the difference in quality of starting materials as-received from the manufacturer.

CHAPTER 4 CONCLUSIONS

Physical, chemical, and thermal properties of the raw materials used to synthesize $CsSrI_3$: Eu were studied in an effort to determine how to overcome the challenges presented by synthesizing this compound. FT-IR was used to detect the presence of impurities within the as-received raw materials, and revealed the presence of either oxygen or moisture impurities in all of the samples. However, the spectra of SrI_2 and EuI_2 also contained evidence of water being present in these materials. Hygroscopicity measurements of these materials showed that SrI_2 was the most hygroscopic material, while CsI was the least hygroscopic. Thermal analysis was used to identify an appropriate drying temperature. There did not appear to be a need to dry CsI, but SrI_2 and EuI_2 iodide demonstrated a need to be dried at a temperature of ~225°C. Samples were synthesized with different drying parameters to determine the merit of various approaches. While it was presumed that the best drying procedure would include the separate drying of the SrI_2 and EuI_2 starting materials, the preliminary results suggest otherwise. This could be a result of the execution of the transfer of the dried materials into a different synthesis ampoule. Undoubtedly, further evaluation of multiple sample sets of the previously outlined drying procedures would enhance this study. Moreover, auxiliary drying temperatures, and stepped drying procedures could be evaluated. The most successful drying regiment for CsSrI3: Eu noted by this work was to dry all raw materials at a vacuum level on the order of 10^{-6} torr for at least 8 hours at a temperature of ~ 225°C as it had the highest light output (54,000 ph/MeV) and best energy resolution (6.7%) as compared to other samples synthesized for this study.

LIST OF REFERENCES

[1] G.F. Knoll, Radiation Detection and Measurement 4ed, John Wiley and Sons, New York, (2010).

[2] P. Lecoq, A. Annenkox, A. Gektin, M. Korzhik, C. Pedrini, Inorganic Scintillators for Detector Systems: Physical Principles and Crystal Engineering, Springer, Verlag, Berlin, Heidelberg, (2006).

[3] N. Cherepy, L. Boatner, A. Burger, K. Shah, S. Payne, A. Janos, A. Kuhn, "Overview of Strontium Iodide Scintillator Materials," LLNL presentation April 1, 2010 (LLNL-PRES-426327).

[4] N. Cherepy, G. Hull, A.D. Drobshoff, S.A. Payne, E. van Loef, C.M. Wilson, K. S. Shah, U.N Roy, A. Burger, L.A. Boatner, W.S. Choong, W.W. Moses, "Scintillators with potential to supersede lanthanum bromide," *Applied Physics Letters,* Vol. 92, (2008) 083508-083503

[5] E.V. van Loef, et. al., "Crystal growth and scintillation properties of strontium iodide scintillators," *IEEE Transactions on Nuclear Science*, Vol. 56 No. 3, (2009) 869-872.

[6] E.D Bourret- Courchesne, G. Bizarri, R. Borade, Z. Yan, S. M. Hanrahan, G. Gundiah, A. Chaudry, A. Canning, S.E. Derenzo, *Nuclear Instrument Methods A*, Vol. 612, (2009) 138-142

[7] E. D. Bourret- Courchesne, G. Bizarri, S.M. Hanrahan, G. Gundiah, Z. Yan, S. E. Dorenzo, *Nuclear Instrument Methods A*, Vol. 613, (2010) 95-97.

[8] E.D. Bourret- Courchesne, G. Bizarri, R. Borade, G. Gundiah, E.C. Samulon, Z. Yan, S. E. Dorenzo, "Crystal growth and scintillation properties of alkali-earth halide scintillators," *Journal of Crystal Growth,*Vol. 352 No. 1, (2012) 78-83.

[9] K. Yang, "Discovery and development of rare earth activated binary metal halide scintillators for next generation radiation detectors," Electronic Thesis submitted to the University of Tennessee, 2011, <http://trace.tennessee.edu/cgi/viewcontent.cgi?article=2240&context=utk_graddiss>.

[10] K. Yang, M. Zhuravleva, C.L. Melcher, "Crystal growth and characterization of $CsSrI_{1-x}Eu_xI_3$ high light yield scintillators," *physica status solidi Rapid Research Letters*, Vol. 5, (2011) 43-45.

[11] G. Bizarri, E. D. Bourret-Courchesne, Z. Yan, S. Derenzo, "Scintillation and Optical Properties of BaBrI: Eu^{2+} and $CsBa_2I_5$: Eu^{2+}," *IEEE Transactions on Nuclear Science*, Vol. 58 No. 6, (2010) 3403-3410.

[12] S. Surti, J.S. Karp, G. Muehllehner, P.S. Raby, "Investigation of Lanthanum Scintillators for 3-D PET," *IEEE Transactions on Nuclear Science,* Vol. 50, No. 3, (2003) 348-354.

[13] W. M. Higgins, A. Churilov, E. van Loef, J. Glodo, M. Squillante, K. Shah, " Crystal Growth of large diameter $LaBr_3$: Ce and $CeBr_3$," *Journal of Crystal Growth,* Vol. 310, (2007) 2085-2089.

[14] Hans J. Scheel, Tsuguo Fukuda, Crystal Growth Technology, John Wiley & Sons, West Sussex, England, (2003) 355.

[15] R. Hofstadter, "Europium activated strontium iodide scintillators," *United States Patent No. 3,373,279,* March 12, 1968.

[16] V.L Cherginets, A. Y. Grippa, T.P. Rebrova, Y. N. Datsko, T.V. Ponomarenko, N. V Rebrova, N.N. Kosinov, O. A. Tarasenko, Y. I. Dolzhenko, O. V. Zelenskaya, "Scintillation properties of Eu^{2+} doped $SrCl_2$ and $CsSrCl_3$ single crystals," *Functional Materials,* Vol. 19 No. 2, (2012) 187-191.

[17] R. C. Ropp, Encyclopedia of the Alkaline Earth Compounds, Elsevier, Oxford, UK, (2013).

[18] E. Samulon, E.D. Bourret- Courchesne, G. Bizarri, "Growth and study of undoped and europium doped BaBrCl scintillator crystals: Impact of oxygen defects on performance," Oral presentation at the 23rd Conference on Crystal Growth and Epitaxy, Fallen Leaf Lake, CA, June 4, 2012.

[19] E. D. Bourret- Courchesne, " Discovery and development of scintillator materials," Oral presentation at the 5th Annual Academic Research Intiative Grantees Conference, Leesburg, VA , September 25, 2012.

[20] J. Bassett, R. C. Denney, G. H. Jeffery, and J. Mendham, Vogel's Textbook of Quantitative Inorganic Analysis, John Wiley & Sons Inc., New York, (1978).
[21] *ChemFiles*Vol. 5 No. 13, Sigma Aldrich, (2005), <<http://www.sigmaaldrich.com/chemistry/chemical-synthesis/learning-center/chemfiles/chemfiles-2004-2005.html>.
[22] R. Thomas, Practical Guide to ICP-MS: A Tutorial for Beginners, CRC Press, Taylor & Francis Group, Boca Raton, FL, (2008).
[23] K. Nakamato, Infrared and Raman Spectra of Inorganic and Coordination Compounds, Part A: Theory and Applications in Inorganic Chemistry, New York, NY: John Wiley and Sons, (1997).
[24] S. C. Jain, A. V. R. Warrier, S. K. Agarwal, "Electronic absorption and internal and external vibrational data of atomic and molecular ions doped in alkali halide crystals," National Standard Data Reference System, U.S. Department of Commerce, (1974).
[25] A. Baraldi, R. Capelletti, N. Chiodini, C. Mora, R. Scotti, E. Uccellini, A. Vedda, "Vibrational spectroscopy of OH-related groups in Ce^{3+} and Gd^{3+} doped silicate glasses," *Nuclear Instruments and Methods in Physics Research A*¸ Vol. 486, (2002) 408-411.
[26] A. Dauletbekova L. Lisitsyna, V. Korepanov, V. Lisitsyn, L. Trefilova, R. Kassymkanova, "Radiation transformation of the oxygen-containing impurity in LiF crystals doped with different polyvalent cations," *physica status solidi C*, Vol. 10 No. 2, (2013) 263-267.
[27] S. Vasyukov, N. Shiran, D. Sofronov, "Scintillation properties deterioration due to hydroxyl and oxygen pressence in Eu doped alkali halides," Poster presentation at the SCINT conference, Shanghai, China, April 2013.
[28] H. H Willard, L.L. Merrit Jr., John A. Dean, Instrumental Methods of Analysis, Van Nostrand Reinhold Company, New York (1948).
[29]G. Höhne (Günther), W Hemminger, H. J. Flammersheim, Differential Scanning Calorimetry 2^{nd} Ed, Springer, New York (2003)
[30] B. W. Strum, N. J. Cherepy, O. B. Drury, P. A. Thelin, S. E. Fisher, S. A. Payne, A. Burger, L. A. Boatner, J. O. Ramey, K. S. Shah, R. Hawrami, "Effects of packaging SrI_2 (Eu) scintillator crystals," *Nuclear Instruments and Methods in Physics Research Section*

A: Accelerators, Spectrometers, Detectors, and Associated Equipment, Vol. 652 No. 1, (2011) 242-246..

[31] Laine, Ensio, Meika Aarnio, "Device for the Investigation of Humidity Related Behaviors of Materials," University of Turku, Finland. http://www.physics.utu.fi/laitos/teollisuusfysiikka/julkaisut/laine1.pdf

[32] B. Blalock, A. Lindsey, H. Wei, "Scintillators: Lighting up the darkness," an Oral Presentation given at the Graduate Student Seminar at the University of Tennessee, Oct. 30, 2012.

[33] G. Schilling, G. Meyer, "Ternäre Bromide und Iodid zweiwertiger Lanthanide und ihre Erdalkali-Analoga vom Typ AMX_3 und AM_2X_5," *Zeitschrift für anorganische und allgemeine Chemie*, Vol. 622, (1996) 759-765.

[34] S. P. Davis, M. C. Abrams, J. W. Brault, Fourier Transform Spectrometry, Academic Press, London (2001).

[35] J. D. Ingle Jr., S. R. Crouch, Spectrochemical Analysis, Prentice-Hall Inc., New Jersey (1988).

[36] P. R. Griffiths, J.A. De Haseth, Fourier Transform Infrared Spectroscopy, Wiley, Hoboken, N.J. (2007).

[37] P. R. Menge, "Performance of large BrilLanCe 380® (lanthanum bromide) scintillators," Oral presentation at the SORMA XI conference, Ann Arbor, MI, May 2006.

[38] L. M. Bollinger, G. E. Thomas, "Measurement of the Time Dependence of Scintillation Intensity by a Delayed- Coincidence Method," *The Review of Scientific Instruments,* Vol. 32 No. 9, (1961) 1044-1050.

[39] E. Buzágh-Gere, et. al. Investigation of dehydration process III Thermal dehydration of strontium iodide hydrates. *Journal of Thermal Analysis,* 17, 501-505 (1979).

[40] S. Podowitz, et. al. Fabrication and properties of translucent SrI_2 and Eu:SrI_2 Scintillator Ceramics. *IEEE Transations on Nuclear Science*, 57, No.6, 3827-3835 (2010).

VITA

Bonnie Dell Blalock was born on August 26, 1983 in Denver, Colorado. She received her Bachelor of Science in Materials Science and Engineering at the University of Tennessee in December of 2011. While still an undergraduate student, she had the incredible fortune of working at the Scintillation Materials Research Center, where she was able to remain working throughout her graduate school experience. Bonnie graduated with a Master of Science degree in December of 2013.